Alma Mater Studiorum - Università di Bologna

SCUOLA DI SCIENZE

Dipartimento di Chimica Industriale "Toso Montanari"

Corso di Laurea Magistrale in

Chimica Industriale

Classe LM-71 - Scienze e Tecnologie della Chimica Industriale

Study of the second hyperpolarizability of poly(3-alkylthiophenes) using the third-harmonic scattering technique

Tesi di laurea sperimentale

CANDIDATO

Elena Battaglini

RELATORE

Prof.ssa Elisabetta Salatelli

CORRELATORE

Prof. Guy Koeckelberghs

Dott.ssa Stien Vertommen

Sessione III

I

ABSTRACT

During the past years, the considerable need in the domain of communications for more potent photonic devices focuses the research activities into the nonlinear optical (NLO) materials which can be used for modern optical switches.

In this regard, a lot of research activities are focused on the organic materials and conjugated polymers which offer more advantages compared to the inorganic ones.

On this matter, poly(3-alkylthiophene) (P3AT), an organic conjugated polymer, can be investigated as potential optical materials with in particular the focus on the NLO properties such as the first- and second-hyperpolarizability, β and γ respectively.

The activities carried out at the Laboratory of Polymer Synthesis of the KU Leuven, during the master's thesis work, focused on the study of conjugated polymers in order to evaluate their NLO properties for the future purpose of applications in optical systems.

In particular, three series of polythiophenes functionalized with an alkyl side chain in the 3-position were synthesized: poly(3-hexylthiophene) (P3HT), poly[3-(2-ethylhexyl)thiophene] (P3EHT) and random copolymer of the two regio-isomers of P3HT. They were made in order to study the influence of molar mass, branching and regio-irregularity on the γ-value. The Kumada catalyst transfer condensative polymerization (KCTCP) and the Pd(RuPhos)-protocol were used for the polymerizations in order to have control over the molar mass of the growing chain and consequently to obtain well-defined and reproducible materials. The P3AT derivatives obtained were characterized by gel permeation chromatography (GPC), spectroscopic techniques (^{1}H-NMR, UV-Vis) and the γ-value was investigated using the third-harmonic scattering (THS) technique. In particular, the THS technique is useful to investigate the optical behavior of the series of polymers in solution. The results obtained point out the difference in NLO behavior, especially the γ-value, between linear, branched and regio-irregular alkyl substituents of P3AT.

SUMMARY

CHAPTER 1: THEORETICAL BACKGROUND

1.1 General aspects of nonlinear optics

1.1.1 Linear interaction of light with matter

The electro-magnetic (EM) radiation is a form of energy that propagates through space at very high speeds. The phenomena related to the absorption and emission of radiant energy rely on a corpuscular model, in which EM radiation is represented as a flow of discrete particles or wave packets called photons, whose energy is proportional to the frequency of the radiation. EM radiation can be described by an electric (E (r, t)) and magnetic (B (r, t)), (r= space, t= time) field that oscillates orthogonally to each other and perpendicular to the direction of propagation. Generally, the electric component of the EM radiation is considered much more than the magnetic component since it is the electric field that is responsible for the most of chemical interesting phenomena.[1]

The electric field component of the EM radiation can be written as:

$$E(r, t) = E_0\left(e^{ik.r - i\omega t} + cc\right)$$

The most important parameters characteristics of the EM radiation are:

- ω = pulsation = $2\pi\nu$ (ν is the frequency)
- k = wave vector = $\frac{2\pi}{\lambda} = \frac{n\omega}{c}$ (λ is the wavelength, n is the refractive index and c is the light speed in vacuum)
- cc is the complex conjugate

Now, the interaction between a dielectric material and EM radiation is considered: the material is normally made up of electrically neutral molecules but

each i-th molecule can have, even if electrically neutral, a charge separation + q and –q at a distance d. This charge separation is defined as an electric dipole (*Figure 1*).
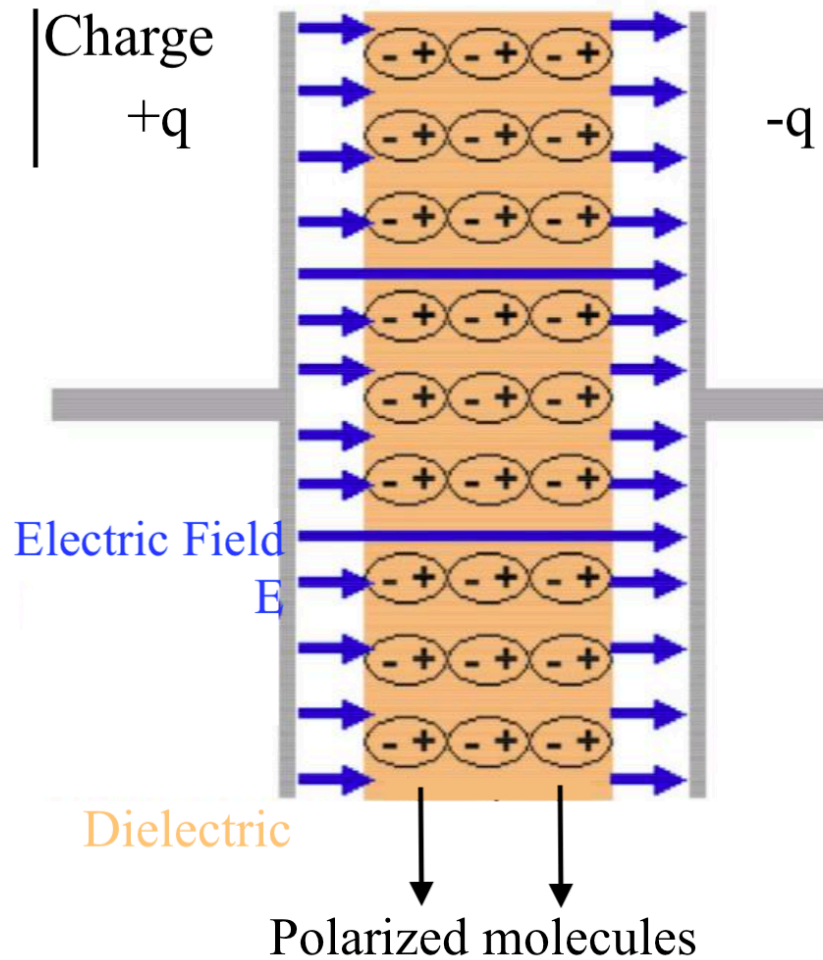
Figure 1. Interaction between electric field and dielectric medium: polarization of the molecules.[2]

These electric properties of the molecules are described by the so-called dipole moment, μ.

$$\mu = q \cdot d$$

When a polar molecule (dipole) approaches a molecule without a static dipole moment there is a charge shift in the non-polar molecule: an induced dipole moment arises (*Figure 2*).

Polar molecule   Apolar molecule   Static dipole   Induced dipole
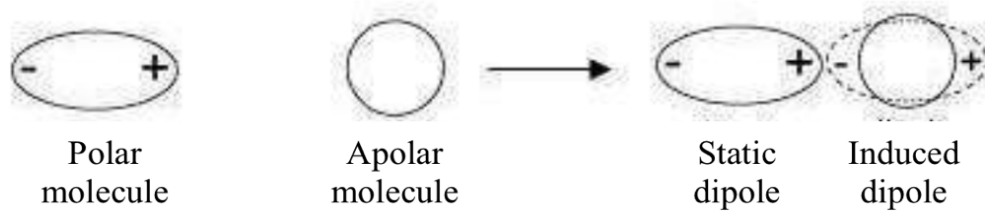
Figure 2. Induced dipole moment.

The same effect occurs when a non-polar molecule is immersed in an electric field which induces a charge separation in the molecule and, consequently, the formation of an induced dipole moment.

The intensity of the induced dipole moment (μ_{ind}) depends on the intensity of the applied electric field (E), according to the equation:

$$\mu_{ind} = \alpha E$$

E is considered as the oscillating electric field component of the EM radiation, so the equation can be written as:

$$\mu_{ind}(\omega) = \alpha(\omega)E(\omega)$$

with $\alpha(\omega)$ the linear polarizability.

The total dipole moment of the molecule (p) is the sum of the induced dipole moments $\mu_{ind}(\omega)$ and the static dipole moment μ:

$$p = \mu_{ind}(\omega) + \mu$$

Instead of considering each molecule apart and working at the microscopic level, you can also work at the macroscopic level and consider an ensemble of molecules. The induced polarization P(ω) is given as the sum of the induced dipole moments of the individual molecules:

$$\left(P(\omega)\right) = \sum_i \mu_{ind}(\omega) = Nf_\omega\alpha(\omega)E(\omega) = \chi^{(1)}(\omega)E(\omega)$$

with $\chi^{(1)}$ the linear susceptibility, N the number density and f_ω a correction factor which depends on the refractive index n_ω at the optical frequency ω.

The following equation relates the $\chi^{(1)}$ to the refractive index n_ω:

$$n_\omega^2 = 1 + 4\pi\chi^{(1)}(\omega)$$

In the event that a dielectric material is absorbent, it is convenient to describe the absorption by adding an imaginary component to the real part of the refractive index (n_1), called the extinction coefficient (k). The refractive index will therefore be represented by the complex size:

$$n = n_1 + ik$$

The real part of the refractive index describes refraction while the imaginary part describes the absorption of light.[3]

1.1.2 Nonlinear interaction of light with matter

In linear optics EM radiation propagates independently of its intensity. Propagation depends only on the wavelength and the speed of light in the material. The equations derived for linear optics, only holds when the intensity is sufficient low. For high intensities, these equations are no longer sufficient, and we have to switch to nonlinear optics.

Nonlinear optics include all those phenomena whereby the polarization of a medium does not vary in a simply linear way with the EM radiation. The discovery of nonlinear optics dates back to Franken's experiment (1961) but it would not have been possible if the technologies of high intensity lasers, capable of stimulating the nonlinearity of materials, had not already been developed.[4]

The invention of lasers which are accomplished by generating monochromatic and coherent light beams at very high speed ($>10^{12}$ W/cm^2), have led to the observation of new physical effects which depend strictly on the intensity of the light and which are described in the scope of nonlinear optics theory.

Each nonlinear optical phenomenon can be summarized in two actions: an optical beam induces a nonlinear response of the medium in which it propagates, and the medium reacts by altering the propagation of the optical field. The electric field of the EM radiation interacts with the electrons in the material and causes a charge separation, leading to an induced dipole moment.

At the macroscopic level, the induced polarization is not proportional anymore to the applied electric field and can be expressed as a Taylor expansion series:

$$P = P^{(1)} + P^{(2)} + P^{(3)} + \cdots = \chi^{(1)} E + \chi^{(2)} EE + \chi^{(3)} EEE + \cdots$$

in which the $\chi^{(n)}$ coefficients are the susceptibility of order n and the $P^{(n)}$ coefficients are the polarizability of order n.

The susceptibilities with n >1 are responsible for the nonlinear behavior of the materials.

Also, when considering the individual molecules, the induced dipole moment in the nonlinear regime can be written as:

$$\mu_{ind} = \mu^{(1)} + \mu^{(2)} + \mu^{(3)} + \cdots = \alpha E + \beta EE + \gamma EEE + \cdots$$

with β the first hyperpolarizability and γ the second hyperpolarizability.

1.1.3 Third-harmonic generation (THG)

Many second-order and third-order nonlinear optical effects can occur. These effects are mainly dependent on the input frequencies and the presence of excited states than can be populated by the action of EM radiation. Third-order interactions can occur in both centrosymmetric and non-centrosymmetric media. In an isotropic medium the second-order nonlinearity is not present ($\chi^{(2)} = 0$).

For third-order nonlinear optics, the most used phenomenon is third-harmonic generation (THG). The process of THG is illustrated in *Figure 3*.
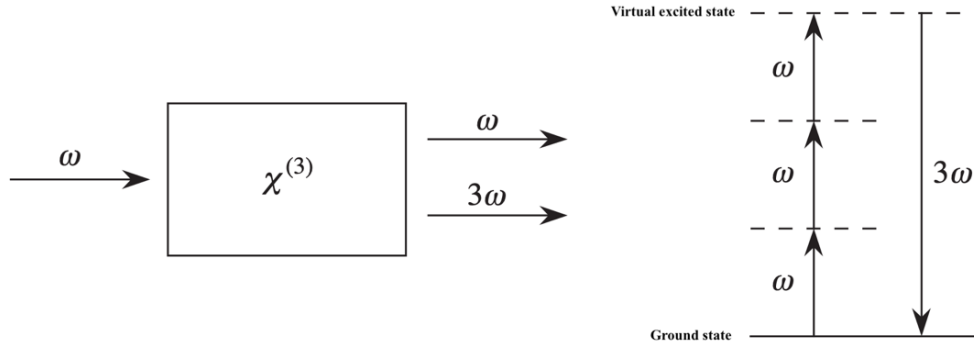
Figure 3. The process of THG. [5]

In this degenerate process three photons of equal energy combine to form a photon at the triple frequency, or at one-third of the wavelength.[5]

The expression of the third-order nonlinear polarization for this type of interaction is given by:

$$P^{(3)}(t) = \chi^{(3)} E(t)^3 = \chi^{(3)} \left(E_0 \bullet \frac{e^{i\omega t} + e^{-i\omega t}}{2} \right)^3$$

$$P^{(3)}(t) = \frac{1}{4} \chi^{(3)} E_0{}^3 \cos(3\omega t) + \frac{3}{4} \chi^{(3)} E_0{}^3 \cos(\omega t)$$

In the above equation it is possible to see two different terms: the first term that oscillates with the triple angular frequency of the applied field, which corresponds to the THG process. The second term which oscillates with the same angular frequency of the applied field, and so, consequently, the material produces as well a radiation which has the same frequency as the incident field and which changes the propagation characteristics.

The linear susceptibility χ is linked to the relative electrical permittivity, ε_r, and to the linear refraction index of the medium, n_0, by the following expression:

$$\chi = \varepsilon_r - 1 = n_0^2 - 1$$

the refractive index is a quantity closely related to the polarizability of the medium. The term $P^{(3)}(t)$, cubic in E_0, causes the beam, while passing through the medium, to instantly change its refractive index n, proportionally to the intensity I (r, t) of the beam itself, according to the law:

$$n = n_0 + n_2 I(r, t)$$

where n_2 is the Kerr coefficient, given by:

$$n_2 = \frac{3}{4\varepsilon_0 c n_0^2} \chi^{(3)}$$

The medium in which this equation is valid is called a Kerr medium.[2]

1.2   THS technique

Third-harmonic scattering (THS) is a technique useful to quantify the molecular second hyperpolarizability (γ-value) and which is based on nonlinear light scattering. THS is an advanced system developed to study the nonlinear optical behavior of organic molecules in solution; it is an innovative technique compared to the precedent method as THG because with THS the γ-value can be determined with high sensitivity and the data analysis is quite simple. In the other methods like THG, z-scan, etc. the working conditions are, in general, more difficult and analysis errors are more frequent.[6]

THS is a non-invasive and very sensitive technique in which the scattered light is detected at the optical frequency of 3ω while the incident beam is pulsed at ω. [7] Three photons, each at an incident frequency of ω are annihilated to create an output photon at the triple frequency 3ω.

In the THS process the laser beam that pass through the sample is scattered over the entire medium as it shown in *Figure 4*.
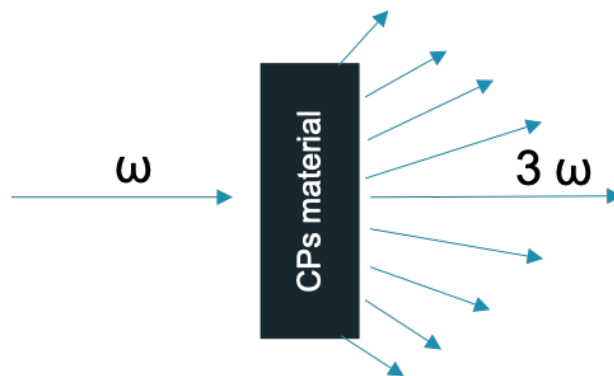
Figure 4. Schematic representation of the THS process.

1.3 Material for NLO

During the past years, the considerable need in the domain of communications for more potent photonic devices focuses the research activities into the nonlinear optical (NLO) materials which can be used for modern optical switches.[8] In this regard, a lot of research activities are focused on the organic materials and conjugated polymers which offer more advantages compared to the inorganic ones.

1.3.1 Conjugated polymers

Polymers began to have a particular interest as possible electricity-conducting materials when in 1977 professors Heeger, McDiarmid and Shirakawa discovered peculiar characteristics of polyacetylene conductivity.[9,10,11,12]

Subsequent studies have made the sector of conductive polymers an important commercial reality especially in the technological field, thanks to the particular characteristics and properties of these new materials.

Intrinsically Conductive Polymers (ICPs) are able to conduct electrical current due to the presence of a system of π double bonds conjugated along the backbone of the macromolecule which generate an electronic delocalization essential for the conductivity of the material. The electrical conductivity achieved in these polymers guarantees their properties both in semiconductors, if they are in a neutral state, and in conductors (metal-like) in the case they are in the doped state. Therefore, they have the advantage of being able to combine the high conductivity, normally reserved for metals, with the intrinsic mechanical properties of polymers, especially their lightness, flexibility, filmability and processability.[13] Moreover, their specific properties, regard also the possibility to easily derivate monomer/polymer with simple structural alteration. The phenomenon of electrical conductivity in conjugated polymers can be explained through the band model, developed for inorganic semiconductors. The main characteristic of the conducting polymers, as mentioned above, is the presence of a conjugated double bond system which determines the formation of delocalized π orbitals along the chain of macromolecules. The π-molecular orbitals, resulting from the interaction between the p-orbitals of sp^2-hybridized carbon atoms, generate two bands, one of "valence" and one of "conduction": the valence band is constituted by the π (bonding) orbitals while the conduction band is constituted by the π^* (antibonding) orbitals.[14] The energy of the highest occupied molecular orbital (HOMO) increases, while the energy of the lowest unoccupied molecular orbital (LUMO) decreases, thus reducing the energy gap (Eg) between the bands, (*Figure 5*).
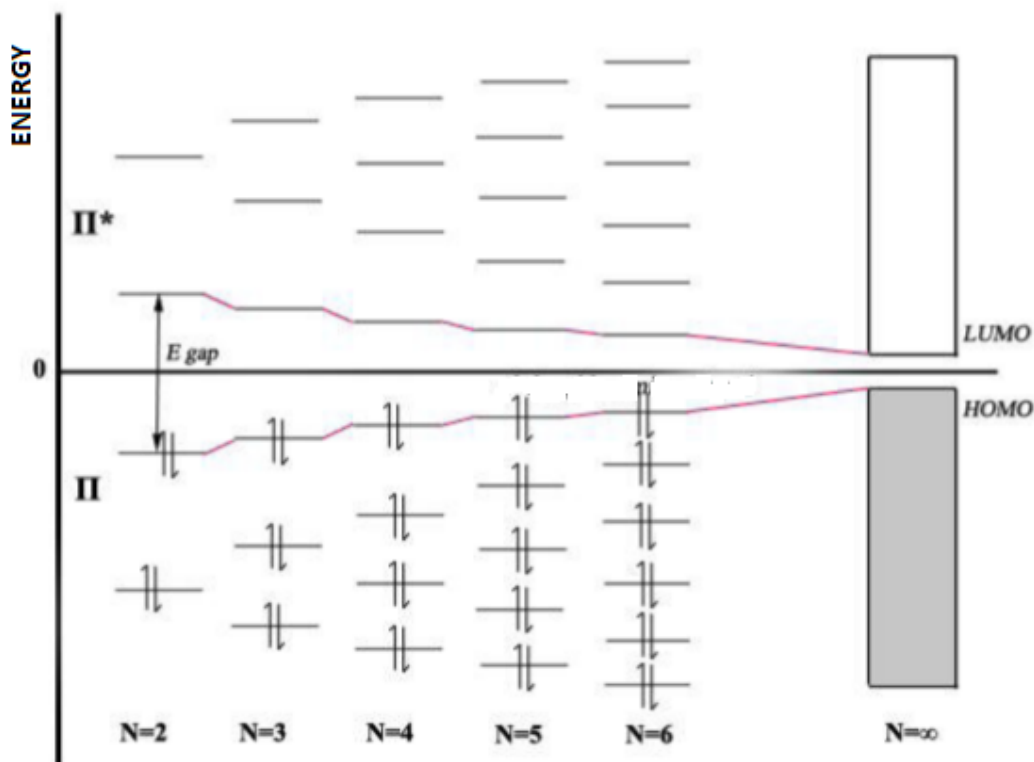
Figure 5. Band gap.[15]

To obtain sufficiently high conductivity values it is necessary to reduce the distance between these two bands (Eg) in order to facilitate the promotion of the excited electrons to the conduction band. Whether the conjugation within the structure increases, the energy gap between the valence band and conduction band decreases and there is an increasing of the material conductivity.

The size of the band gap and the position of the HOMO and LUMO energy levels are therefore the most important characteristics for determining the optical and electrical properties of the conjugated polymers.[16,17]

In this regard, polythiophene (PT) and its derivates increase their attractiveness due to their chemical and physical properties.

1.3.2 Polythiophenes

PT is one of the most studied conjugated polymers due to its interesting properties, in particular its high conductivity and stability.

However, it does not appear to be a particularly suitable material to be processed and formed due to its insolubility in common organic solvents because of the strong π-π interaction. Some studies have shown the existence of tricks aimed at improving the poor workability of the PT.[18] In particular, it has been discovered that through the addition of certain substituents in 3-position of the thiophene, the polymer becomes soluble and filmable.

In the event that the substituent is an alkyl chain, a poly(3-alkylthiophene) (P3AT) is obtained. The alkyl side chain decreases the solid-state packing due to the π-stacking of the aromatic rings, making the polymer soluble and well filmable. In this way the coplanarity of the aromatic rings is reduced due to the steric hindrance introduced by the alkyl side chain itself. This affects negatively the delocalization charge along the polymer chains and the relative final conductivity. The length of the alkyl substituent, in terms of numbers of carbon atoms, has a considerable importance: an excessively small side chain would not give acceptable solubility, while an excessively extended chain would dilute the electronic properties of the conjugated polymer backbone.

1.3.3 Regio-regular P3AT

Regio-regular P3AT can be obtained due to the asymmetric nature of the monomer unit. In general, three different orientations can be achieved due to the coupling between the 2- and 5-position of the thiophene ring.

The three different possible triads of regio-isomers are shown in *Figure 6* and they are namely head-to-tail (HT) (2- 5 '), tail-to- tail (TT) (5-5') and head-to-head (HH) (2-2 ') coupling.[19,20]
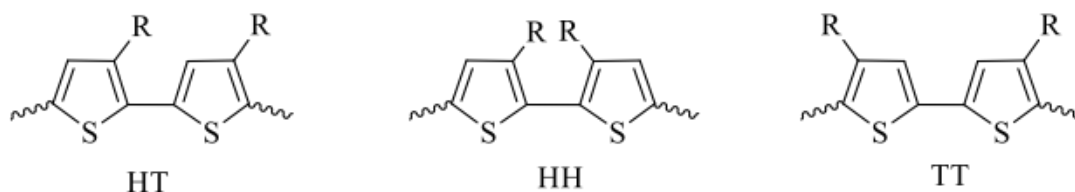

Figure 6. Triads of regio-isomers.

The different types of couplings can create problems related to the extension of the average conjugation in the polymer chain and therefore problems related to the electronic properties of the polymer, as these depend on the conjugation.

In fact, a TT or HH coupling involves deviations from the co-planarity between two adjacent monomeric units due to the steric hindrance induced by the lateral alkyl chains. This situation implies a smaller extension of the average conjugation length along the chain and, consequently, a worse electronic delocalization.[21,22]

1.4 Controlled polymerization

Controlled polymerization has always attracted attention by the scientific community and certainly when McCullough [23] and Yokozawa acknowledged a chain-growth method. This discovery changed the research activity in the field of polymer synthesis.[24] The ability to control growth and termination of polymer chains is a useful instrument to build an innovative material with clear characteristics.

In a chain-growth polymerization the degree of polymerization and the molar mass of the polymer is predictable by the monomer over initiator ratio. Moreover, it is also possible to control the end groups of the polymeric chain which can be critical for certain applications of conjugated polymers.[25]

1.4.1 Kumada catalyst transfer condensative polymerization (KCTCP)

KCTCP is one example of a controlled polymerization technique and is mostly used. Each initiator molecule starts exactly one polymer chain whereby the molar mass can be predicted through the formula $M_n = [M]_0/[I]$, provided that the initiation step proceeds faster than the propagation reaction.

The polymerization synthesis develops in a sequence of oxidative addition (OA), transmetallation (TM) and reductive elimination (RE) catalyzed by a transition metal catalyst.[26,27,28]

The polymerization follows a chain-growth mechanism, and this is due to the fact that the catalyst always remains associated with the π system of the polymer chain during RE. The catalyst remains complexed to the polymer chain after RE. Then it is transferred to the C-Br bond of the terminal monomer unit where OA occurs. Afterward, a TM occurs where the next monomer unit is coupled to the growing polymer chain. This cycle repeats several times in order to obtain a polymer. The polymerizations that follow this type of association to obtain a controlled chain-growth process are called catalyst transfer polymerization (CTP).

In the case of KCTCP, the reaction mechanism involves a cross coupling reaction (Kumada coupling) between an organomagnesium reagent and an organic halide. The most used catalysts in CTP are Ni- and Pd-based; the former catalyst gives rise to a higher degree of control over the polymerization but it can depend on the functionalities of the monomeric units. Therefore, the main problem with Pd-catalysts, in KCTCP, are the weaker association with the polymer backbone compared to their Ni counterparts.[29,30]

When $Ni(L_2)X_2$ is used as a catalyst the polymerization starts with two consecutives TM steps between the catalyst and two monomers units, as shown in *Scheme 1*.
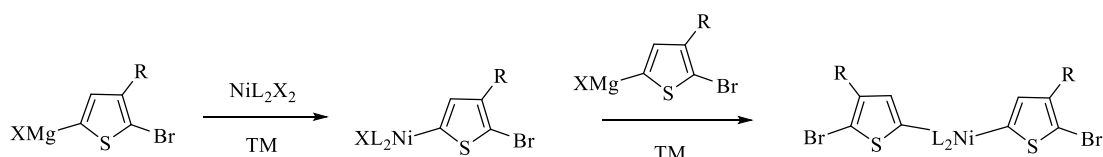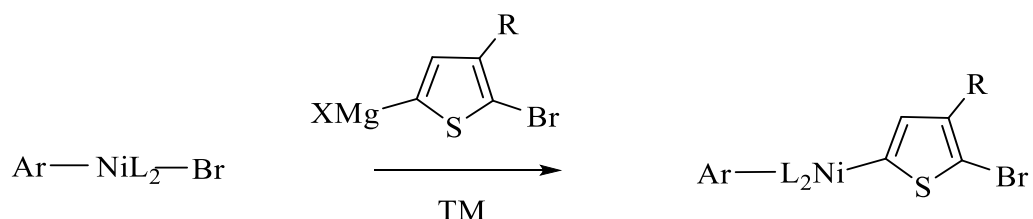

Scheme 1. Initiation step when using $NiXL_2$ as catalyst.

Afterward a dimer is formed by the RE step and the following OA occurs intramolecularly in one of the two C-Br bonds. (*Scheme 2*).
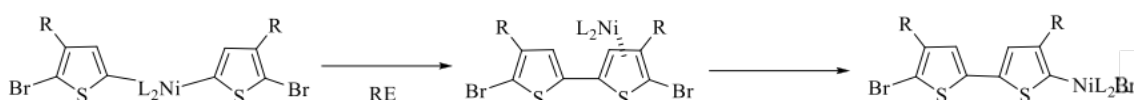

Scheme 2. RE and OA when using NiL_2X_2 as catalyst.

Instead of using a catalyst, an external initiator can also be used to initiate the polymerization. In this case the initiation starts with one TM between the catalyst and a monomer unit. The reactive ligand is incorporated at the beginning of each polymer chain, as shown in *Scheme 3*.

Scheme 3. Initiation step when using an external initiator.

Afterward the consecutives steps are the same as before, a RE step followed by an OA. (*Scheme 4*).
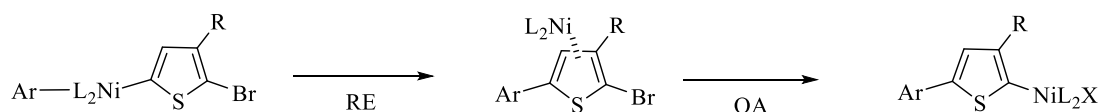
*Scheme 4. RE and OA when using an external initiator.*

Both the initiator and the Grignard reagent are extremely sensitive towards oxygen and humidity, so it is very important to control the reaction conditions and the Grignard reagent is prepared *in situ*, just before the polymerization.

Ligands play a fundamental role in the control of a chain-growth polymerization. In fact, the organization around the centre of the metal is particularly important. Ligands as (1,3-bis(diphenylphosphino)propane) (dppp), which is a bidentate ligand, provide greater control over the polymerization compared to monodentate ligands such as triphenylphosphine (PPh$_3$).

Dppp has a larger bite angle which offers a better interaction between the catalyst and the monomer.[30,31]

1.4.2 Pd(RuPhos)-protocol

The Pd(RuPhos)-protocol is another example of a controlled polymerization technique. The controlled character of the polymerization relies on monomer deactivation, while with KCTCP the catalyst association is responsible for the controlled character. The Pd(RuPhos) protocol involves a cross coupling reaction between an organozinc reagent and an organic halide. The organozinc function deactivates the halide function, so OA cannot happen. To initiate the polymerization, a Pd(RuPhos) catalyst is used. The initiator is chosen similar to the monomer unit, but without the deactivating organozinc function. The synthesis of the initiator is shown is *Scheme 5*.
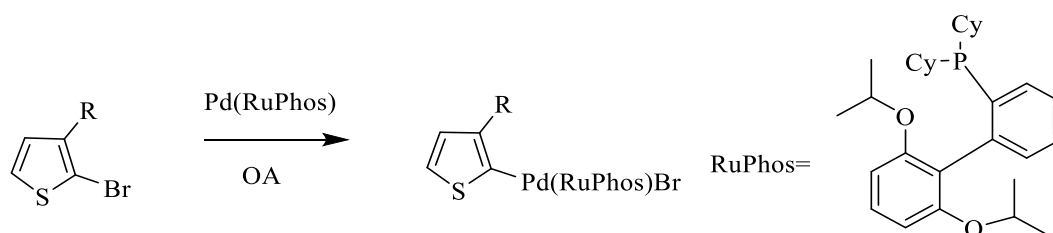
Scheme 5. Preparation of initiator.

The polymerization starts with a TM between the initiator and the bromozinc functionalized monomer, as shown in *Scheme 6*.
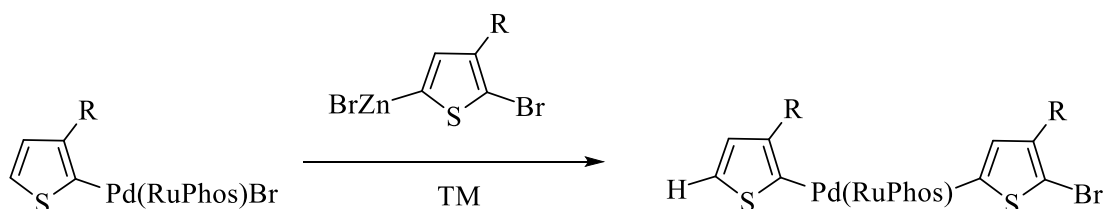
Scheme 6. Transmetallation.

Afterward, a dimer is formed by a RE and the following OA occurs between the catalyst and the formed dimer due to the presence of a C-Br free bond at the end of the polymer chain; then by the addition of new monomer units the polymerization proceed until termination (*Scheme 7*).[30]
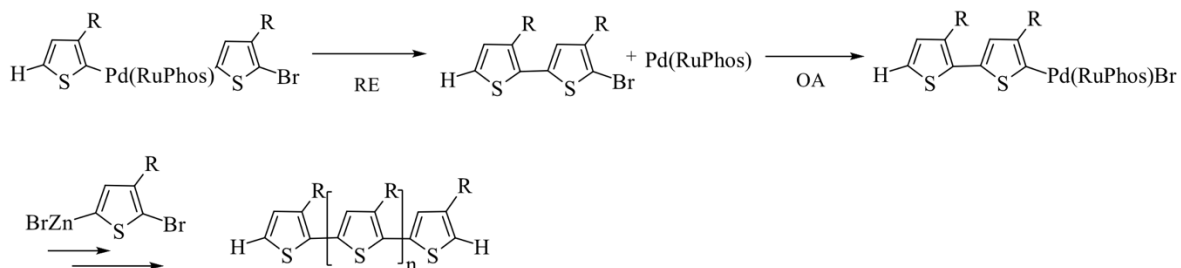
Scheme 7. Reductive Elimination and Oxidative Addition.

Bibliography of Chapter 1

1. Douglas A. Skoog, James J. Leary; Strum. Anal. Chem., (2000).
2. Assimo Maris; Principi di Laser, (2019).
3. Verbiest, T., Clays, K., Rodriguez, V.; Second-Order Nonlinear Optical Characterization Techniques; Taylor & Francis Inc, (2009).
4. Y. R. Shen; "The principles of nonlinear optics"; Wiley-Interscience (2002).
5. R. W. Boyd; "Nonlinear Optics"; Academic Press.
6. Nick Van Steerteghem, Koen Clays, Thierry Verbiest, and Stijn Van Cleuvenbergen; Third-Harmonic Scattering for Fast and Sensitive Screening of the Second Hyperpolarizability in Solution; Anal. Chem. 89, 2964−2971, (2017).
7. J. S. Ford and D. L. Andrews; Molecular Tensor Analysis of Third-Harmonic Scattering in Liquids; J. Phys. Chem. A, 122, 563−573, (2018).
8. Christian Rothe, David Neusser, Niklas Hoppe, Klaus Dirnberger, Wolfgang Vogel, Sergio Gámez-Valenzuela, Juan T. López Navarrete, Belén Villacampa, Manfred Berroth, M. Carmen Ruiz-Delgado, Sabine Ludwigs; Push-pull thiophene chromophores for electro- optic applications: from 1D linear to β- branched structures; Phys. Chem. Chem. Phys., (2020).
9. H. Shirakawa, E. J. Louis, A. G. MacDiarmid, C. K. Chiang, A. J. Heeger, J.; Synthesis of electrically conducting organic polymers: halogen derivates of polyacetylene $(CH)_x$; Chem. Soc. Chem. Comm., 578-580, (1977).
10. Rasmussen, S. C.; Electrically conducting plastics: Revising the history of conjugated organic polymers; ACS Symposium Series; 1080, 147–163, (2011).
11. Hideki, S., Louis, E. J., MacDiarmid, A. G., Chiang, C. K. & Heeger, A. J. Synthesis of Electrically-Conducting organic Polymers: Halogen

Derivatives of Polyacetylene, (CH)x; J.C.S., Chem. Commun. 0, 1–5, (1977).

12. Chiang, C. K., Fincher, C. R., Park, Y. W., Heeger, A. J., Shirakawa, H., Louis, E. J., Gau, S. C., MacDiarmi, A G. Electrical conductivity in doped polyacetylene; Phys. Rev. Lett. 39, 1098–1101, (1977).

13. Coakley, K. M. & McGehee, M. D. Conjugated polymer photovoltaic cells; Chemistry of Materials 16, 4533–4542, (2004).

14. Moliton, A. & Hiorns, R. C.; Review of electronic and optical properties of semiconducting-conjugated polymers: Applications in optoelectronics; Polym. Int. 53, 1397–1412, (2004).

15. Baccolini Gessica, Lanzi Massimiliano; Sintesi e caratterizzazione di nuovi politiofeni idrosolubili per applicazioni fotovoltaiche; (2014-2015).

16. Hilberer, A. et al; Photonic Materials for Electroluminescent, Laser and Photovoltaic Devices; Macromol. Symp. 1, 99–109 (1997).

17. David Bloor; Electrical Conductivity; (1989).

18. Thaneshwor P. Kaloni, Patrick K. Giesbrecht, Georg Schreckenbach and Michael S. Freund; Polythiophene: From Fundamental Perspectives to Applications; Chem. Mater.; 29, 10248−10283, (2017).

19. McCullough, R. D., Williams, S. P., Tristramnagle, S., Jayaraman, M., Ewbank, P. C., Miller, L.; The First Synthesis and New Properties of Regioregular Head-to-tail Coupled Polythiophenes; Synthetic Metals; 69 (1-3), 279-282, (1995).

20. McCullough, R. D., Lowe, R. D.; Enhanced electrical conductivity in regioselectivity synthesized poly(3-alkylthiophenes); Journal of the Chemical Society, Chemical Communications; (1), 70-72, (1992).

21. E. González-Juárez, M. Güizado-Rodríguez, V. Barba, M. Melgoza-Ramírez, M. Rodríguez, G. Ramos-Ortíz, J.L. Maldonado; Polythiophenes based on pyrene as pendant group: Synthesis, structural characterization and luminescent properties; Journal of Molecular Structure, (2015).

22. Itaru O. and Richard D. MCC.; Advances in Molecular Design and Synthesis of Regioregular Polythiophenes; 1202-1214, (2008).

23. Sheina, E. E.; Liu, J. S.; Iovu, M. C.; Laird, D. W.; McCullough, R. D.; Chain Growth Mechanism for Regioregular Nickel-Initiated Cross-Coupling Polymerizations; Macromolecules, 37, 3526−3528, (2004).

24. Zachary J. Bryan and Anne J. McNeil; Conjugated Polymer Synthesis via Catalyst-Transfer Polycondensation (CTP): Mechanism, Scope, and Applications; Macromolecules, 46, 8395−8405, (2013).

25. J. Patrick Lutz, Matthew D. Hannigan, Anne J. McNeil; Polymers synthesized via catalyst-transfer polymerization and their applications; Coordination Chemistry Reviews 376, 225–247, (2018).

26. Bryan, Z. J. & McNeil, A. J. Conjugated polymer synthesis via catalyst-transfer polycondensation (CTP): Mechanism, scope, and applications. Macromolecules 46, 8395–8405, (2013).

27. Yokoyama, A., Miyakoshi, R. & Yokozawa, T.; Chain-Growth Polymerization for Poly(3-hexylthiophene) with a Defined Molecular Weight and a Low Polydispersity. Macromolecules 37, 1169–1171, (2004).

28. Tamao, K. et al.; Nickel-Phosphine Complex-Catalyzed Grignard Coupling. I. Cross- Coupling of Alkyl, Aryl, and Alkenyl Grignard Reagents with Aryl and Alkenyl Halides: General Scope and Limitations; Bulletin of the Chemical Society of Japan 49, 1958–1969, (1976).

29. Huddleston, N. E., Sontag, S. K., Bilbrey, J. A., Sheppard, G. R. & Locklin, J.; Palladium-mediated surface-initiated Kumada catalyst polycondensation: A facile route towards oriented conjugated polymers; Macromol. Rapid Commun. 33, 2115– 2120, (2012).

30. Koeckelberghs, G., Hardeman, T., Van Den Eede, M.-P. & Verheyen, L. Controlled synthesis of conjugated polymers and block copolymers; Polymer 108, 97–132, (2016).

31. Wu, S., Huang, L., Tian, H., Geng, Y. & Wang, F.; LiCl-promoted chain growth kumada catalyst-transfer polycondensation of the 'reversed' thiophene monomer; Macromolecules, 44, 7558–7567, (2011).

CHAPTER 2: AIM OF THE PROJECT

Conjugated polymers have received a lot of attention as third-order nonlinear optical (TONO) materials due to their strong extended π-system. Despite the fact they have an inherent large TONO response, practical applications are not feasible yet due to unoptimized conjugated polymers. In this project, we want to reach a first step in optimizing the TONO response in conjugated polymers by investigating several parameters (molar mass, branching, and regioregularity) that can have an influence on the TONO response of conjugated polymers.

Therefore, this work investigates the nonlinear optical properties of a well-known conjugated polymer, PT, with a particular interest on the second hyperpolarizability, the γ-value.

To investigate the influence of the molar mass on the γ-value, a series of poly(3-hexylthiophene) (P3HT) with different degrees of polymerization (DP), is synthesized.

Besides this, another series of poly[3-(2-ethylhexyl)thiophene](P3EHT) with different DP, is synthesized as well. By realizing a small change in the sidechain of the thiophene monomer, the influence of branching on the γ-value can be investigated by comparing P3HT with P3EHT.

At last, the research will be extended by studying also the influence of regio-regularity on the TONO response. Therefore, a series of a random copolymer, with a defined DP, of the two regio-isomers of P3HT is synthesized by varying the ratio of the two regio-isomers. In this way, a series of P3HT with a different percentage of regio-regularity is realized.

After the synthesis of the polymers, the influence of the different parameters on the TONO response is investigated with the THS technique. In this way, we can provide information on the γ-value and make a comparison between the different synthesized series of polymers.

CHAPTER 3: RESULT AND DISCUSSION

3.1 Synthesis of the precursor monomers

3.1.1 Synthesis of 2-bromo-3-(2-ethylhexyl)-5-iodothiophene

The synthesis of the precursor monomer 2-bromo-3-(2-ethylhexyl)-5-iodothiophene occurred as shown in *Scheme 8*. The first step was the formation of the Grignard reagent which was prepared by the reaction of reactive Mg on the alkyl halide in diethylether (Et$_2$O). This Grignard reagent was attached to the thiophene via a Kumada coupling, resulting in 3-(2-ethylhexyl) thiophene. Then, it was brominated with N-bromosuccinimide (NBS) to form 2-bromo-3-(2-ethylhexyl)thiophene. Finally, it was iodinated with I$_2$ and PhI(AcO)$_2$ that requires full conversion and the precursor monomer was purified via column chromatography.[1]
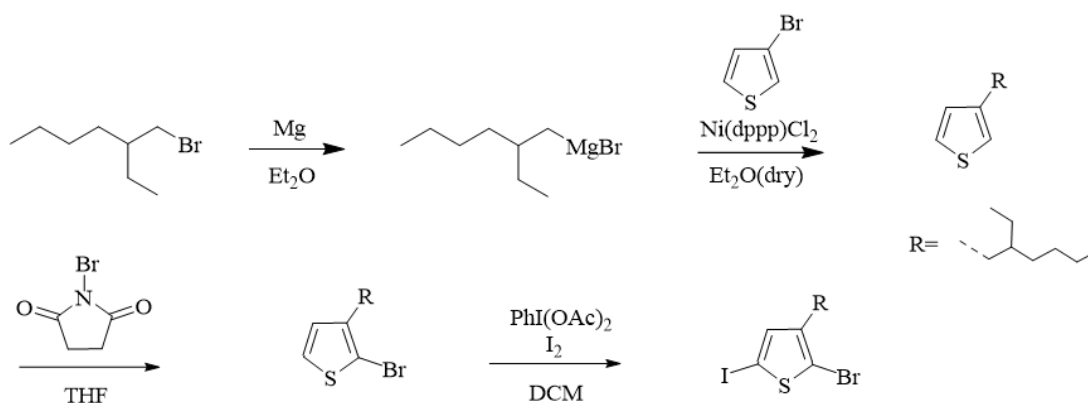
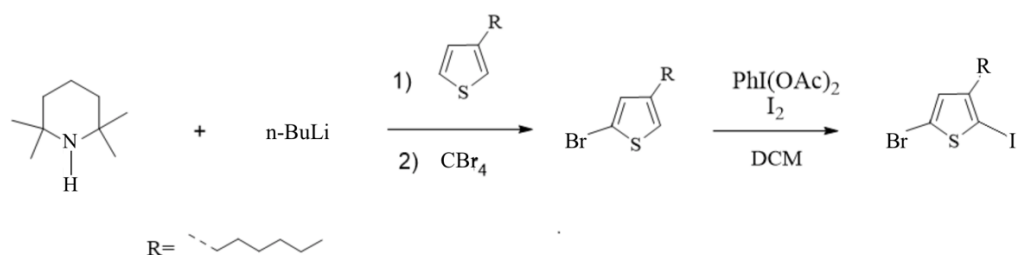*Scheme 8. Synthesis of 2-bromo-3-(2-ethylhexyl) -5-iodothiophene.*

3.1.2 Synthesis of 5-bromo-3-hexyl-2-iodothiophene

The synthesis of the precursor monomer 5-bromo-3-hexyl-2-iodothiophene occurred as shown in *Scheme 9*.

In the first step, the 5 position of the 3-hexylthiophene was brominated by first deprotonating the 5-position using *in situ* prepared tetramethyl piperidinyl

lithium and consequently adding CBr$_4$ to the reaction mixture to get 5-bromo-3-hexylthiophene.

Afterward, it was iodinated with I$_2$ and PhI(AcO)$_2$ in dichloromethane (DCM) as solvent. At last, the precursor monomer is purified via column chromatography.[1]
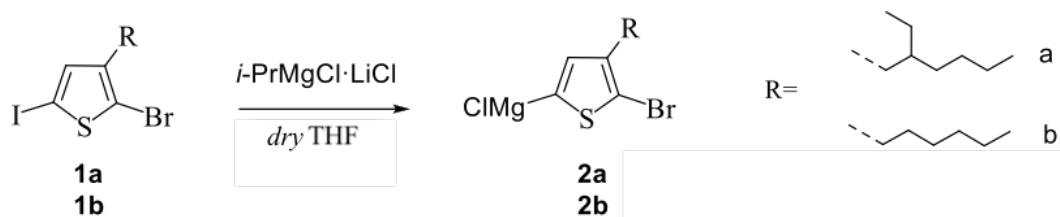

Scheme 9. Synthesis of 5-bromo-3-hexyl-2-iodothiophene.

The 2-bromo-3-hexyl-5-iodothiophene was purchased from TCI and it was used without further purification for the polymerization of P3HT and the regio-irregular P3HT.

3.2   Synthesis of the monomers

3.2.1   Synthesis of 2-bromo-5-chloro magnesium-3-(2-ethylhexyl)thiophene (2a) and 2-bromo-5-chloro magnesium-3-hexylthiophene (2b)

Just before polymerization, the precursor monomers (1a, 1b) were converted into the monomers (2a, 2b) by adding 0.98 equivalent of *i*-PrMgCl·LiCl (*Scheme 10*). The reactivity of the carbon-iodine bond ensures a selective Grignard metathesis (GRIM) reaction in which the iodine atom was exchanged for magnesium chloride.[2]

Scheme 10. GRIM for monomers production.

3.2.2 Synthesis of (5-bromo-3-hexylthiophene-2-yl)zinc bromide and (2-bromo-3-hexylthiophene-2-yl)zinc bromide

Just before polymerization, the precursor monomers were converted to the magnesium chloride monomers by a GRIM reaction using t-BuMgCl in dry tetrahydrofuran (THF) (*Scheme 11*). After 1 hour of reaction the Grignard compounds were reacted with dried $ZnBr_2$ in order to obtain the equivalent organozinc monomers.
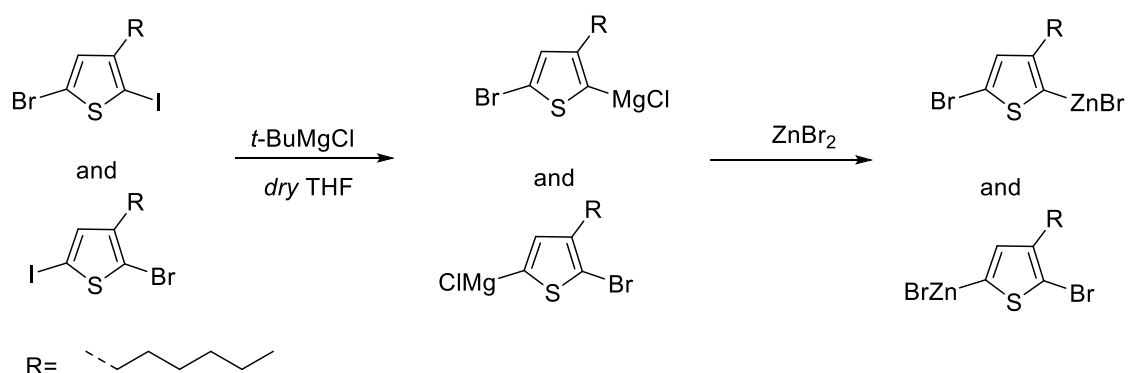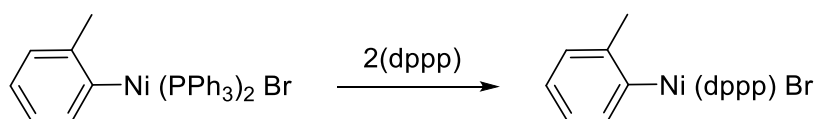

Scheme 11. Synthesis of (5-bromo-3-hexylthiophene-2-yl)zinc bromide and (2-bromo-3-hexylthiophene-2-yl)zinc bromide.

3.3 Synthesis of the external initiator

3.3.1 Synthesis of (o-tolyl)-Ni(dppp)Br

The initiator used for the polymerization was the (*o*-tolyl)-(1,3-bis(diphenylphosphino)propane)bromonickel [(*o*-tolyl)-Ni(dppp)Br] that was prepared *in situ* just before the polymerization (*Scheme 12*).

The precursor initiator, (*o*-tolyl)-Ni(PPh$_3$)$_2$Br, was already present and was synthesized according to the experimental procedure found in the article "Incorporation of Different End Groups in Conjugated Polymers Using Functional Nickel Initiators".[3] As shown in *Scheme 5*, the (*o*-tolyl)-Ni(dppp)Br was prepared by a ligand exchange with 2 equivalents of dppp. Dppp is a bidentate ligand which is useful for the selectivity of the controlled polymerization.

Scheme 12. (o-tolyl)-Ni(dppp)Br initiator.

3.3.2 Synthesis of 2-dicyclohexylphosphino-2′,6′-diisopropoxybiphenyl, (RuPhos) initiator

The initiator was synthesized by the overnight reaction of Pd$_2$(dba)$_3$, RuPhos and 2-bromo-3-hexylthiophene in dry toluene as shown in *Scheme 13*. After the precipitation and the filtration, the presence of the initiator was checked using ^{1}H-NMR. The initiator was in the filtrate solution and not directly in the precipitate powder, so it was purified via column chromatography and the volume was reduced under reduced pressure to obtain a powder.
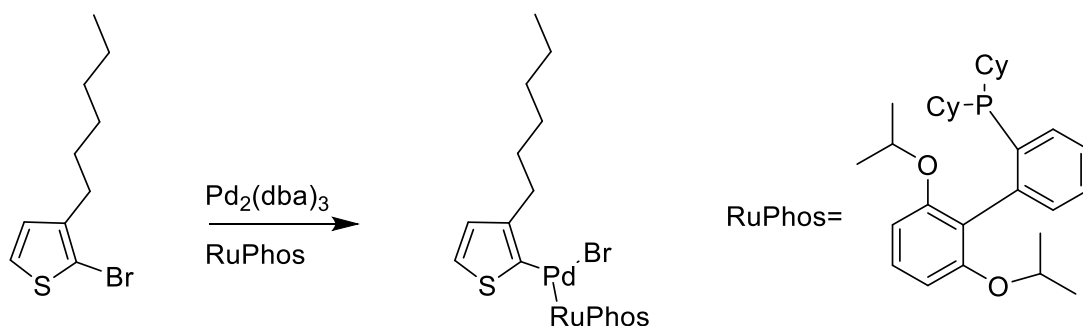
*Scheme 13. Synthesis of Pd(RuPhos) initiator.*

3.4   Synthesis of the polymers

3.4.1   Synthesis of P3HT and P3EHT

The KCTCP started when the monomer and the initiator were mixed in a polymerization tube as shown in *Scheme 14*. The reaction was left to react for 1 hour. Afterward, it was terminated by adding acidified THF, (HCl, 37%). A series of polymers with a varying molar mass was prepared to analyze to the influence of the molar mass on the γ-value. The molar mass can be varied by using the formula:

$$DP = \frac{[Monomer]_0}{[Initiator]}$$

Once the DP was decided, the right amount of initiator and monomer can be calculated.
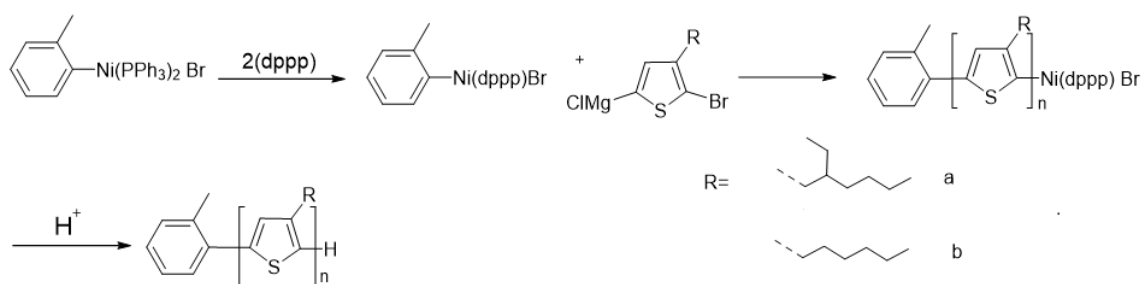
Scheme 14. Polymerization of P3EHT and P3HT.

At the end of the reaction the mass average molar mass ($\bar{M}_w$), number average molar mass ($\bar{M}_n$) and dispersity (Đ) were checked using the gel permeation chromatography (GPC), and all the values are detailed in *Table 1* for the P3HT series and *Table 2* for the P3EHT series. The results obtained from GPC must be interpreted with some carefulness. In this study, polystyrene standards were used as a reference and at the same molar mass, the hydrodynamic volume of the three series of polymer are different compared to the hydrodynamic volume of the reference. So, the molar masses are not-well estimated.

Therefore, the DP can be calculated from the $\bar{M}_n$ and $\bar{M}_w$ determinated via GPC but it is appropriated to use a more absolute method such as ^{1}H-NMR.

Table 1. GPC data of P3HT series.

DP (^{1}H-NMR)	$\bar{M}_n$ (kg/mol)	$\bar{M}_w$ (kg/mol)	Đ
13	2.6	3.1	1.2
15	3.0	3.5	1.2
24	5.2	5.8	1.1
28	6.4	7.4	1.2
37	9.5	10	1.1
41	9.4	10	1.1
45	11	12	1.1
55	13	15	1.1
70	16	19	1.2

Table 2. GPC data of P3EHT series.

DP (^{1}H-NMR)	$\bar{M}_n$ (kg/mol)	$\bar{M}_w$ (kg/mol)	Đ
18	3.5	3.9	1.1
23	5.5	6.2	1.1
29	7.0	8.1	1.2
39	9.5	11	1.1
45	9.5	11	1.2
48	10.8	12.7	1.2
60	12.3	14.8	1.2
71	15.6	19.1	1.2
78	13.6	16.4	1.2

3.4.2 Synthesis of regio-isomer of P3HT

The polymerization started when the monomers, mixed together in the right amount (as describe in the experimental procedure), and the initiator were mixed in a polymerization tube, as shown in *Scheme 15*. For the polymerization it was necessary to have really dried reaction conditions; for this reason, the reagents and the glassware were dried very well before starting. The polymerization was left to react for 1 hour. Afterward, it was terminated by adding acidified THF, (HCl, 37%). For this series of polymers, it was tried to obtain P3HT with different degrees of regioregularity to investigate the optical performance of them.
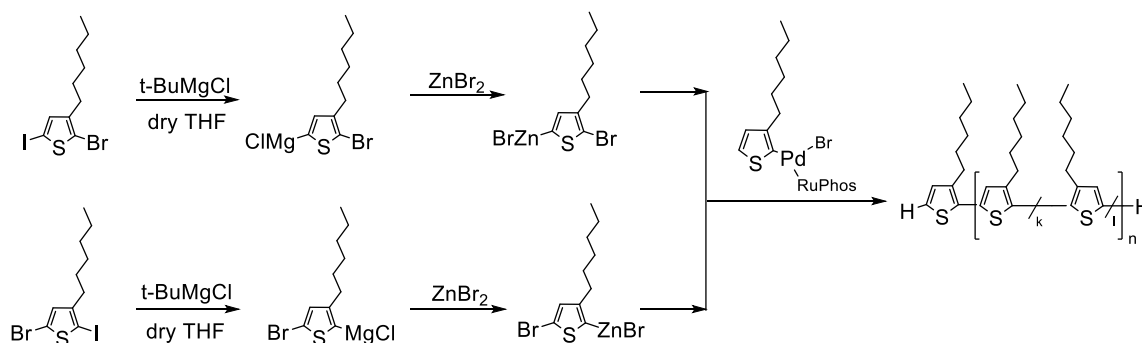
Scheme 15. Synthesis of regio-isosomers of P3HT.

The DP were controlled by using the formula:

$$DP = \frac{[Monomer]_0}{[Initiator]}$$

For this series of polymers, a DP of ~25 was used and also a fixed amount of the two precursor monomers, the 2-iodo-5-bromo-3-hexylthiophene (M2) and the 2-bromo-5-iodo-3-hexylthiophene (M1) was used. As it was said before, at the end of the polymerization the $\overline{M}_n$, $\overline{M}_w$ and the Đ were checked using GPC (*Table 3*). It is also appropriated to use a more absolute method such as ^{1}H-NMR to define the DP.

It was necessary to purified and precipitated again one of the 5 polymers (P3) because from the ^{1}H-NMR there was still RuPhos in the polymer precipitated.

Table 3. GPC data and fixed amount of regio-isomers of P3HT.

Polymer	M1 (mg)	M2 (mg)	DP (^{1}H-NMR)	$\bar{M}_n$ (kg/mol)	$\bar{M}_w$ (kg/mol)	Đ
P1	224	0	25	4.0	5.5	1.4
P2	181	6	23	3.6	5.2	1.4
P3	177	9	25	3.7	5.2	1.4
P4	168	19	23	3.2	4.5	1.3
P5	93.3	93.3	23	3.0	4.1	1.4

Then, for this series of polymers the amount of regio-regularity (*Table 4*) of each polymer was determined by using the method developed by *Barbarella et al.*[4] In this method they had assigned the aromatic region of the ^{1}H-NMR spectrum of the four different possible structural combinations as shown in *Figure 7*.
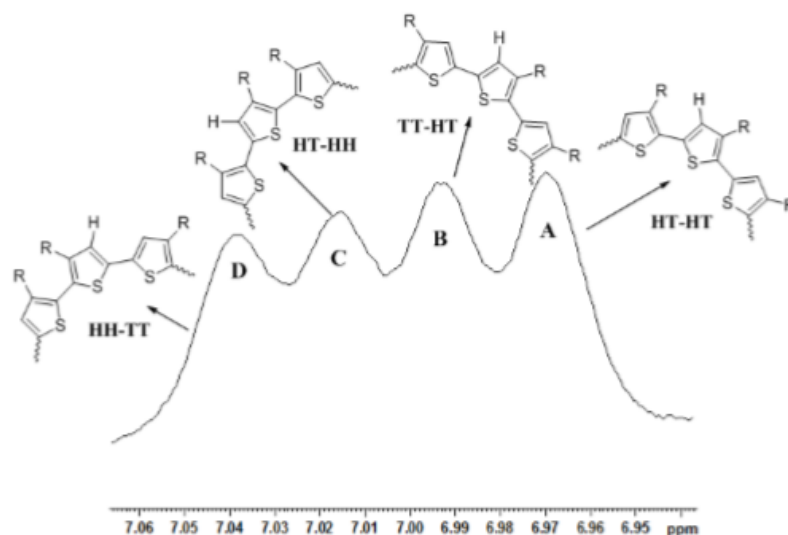

Figure 7. ^{1}H-NMR assignment of the different triads. Figure take from the article: P3AT with tuneable regioregularity: synthesis and self-assembling properties; Willot et al. [5]

For each polymer the aromatic region of the ^{1}H-NMR spectra was integrated, and a deconvolution was performed as shown in *Figure 8*.
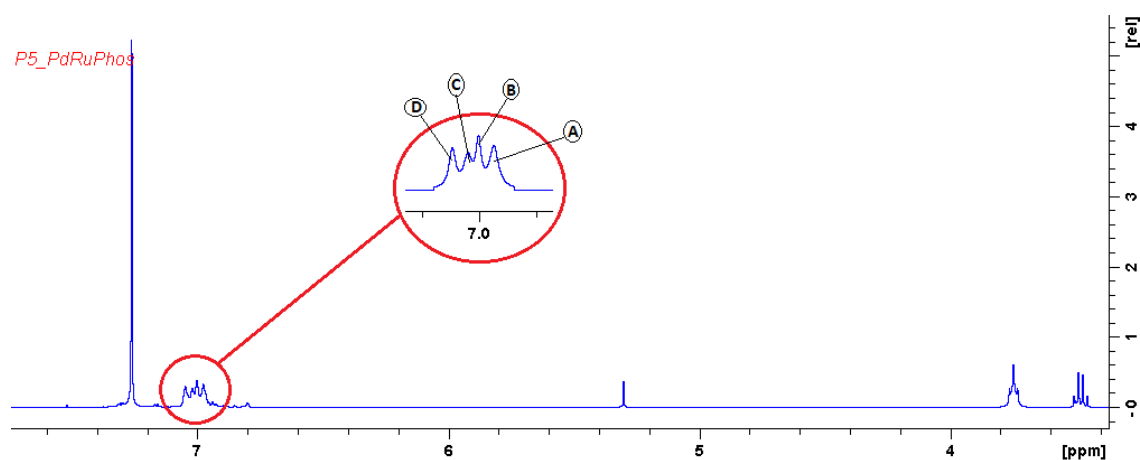

Figure 8. ^{1}H-NMR P5, example of aromatic region from the polymer synthetized in this work.

Then based on the integration of the different peaks, the percentage of regio-irregularity in each polymer was calculated using next formulas:

$$\%HT = \frac{2A + B + C}{2(A + B + C + D)}$$

$$\%HH = \frac{C + D}{2(A + B + C + D)}$$

$$\%TT = \frac{B + D}{2(A + B + C + D)}$$

The A, B, C and D indicate the integral area of each peaks of the respective ^{1}H-NMR spectra.[5]

31

Table 4. Amount of regioregularity of P3HT series.

Polymer	% HT	% TT	% HH
P1	96	1.06	2.94
P2	89.6	4.8	5.6
P3	83	9.1	7.9
P4	81.3	9.1	9.6
P5	55.24	22.12	22.64

For this series of polymers, it was possible to see a trend which links the values of $\overline{M}_n$ with the regio-regularity: the value of $\overline{M}_n$ decreases with the increase of the regio-irregularity. Under the same reaction conditions (polymerization time, temperature etc.) we can see this trend due to the fact that, in this study, polystyrene standards were used as a reference and at the same molar mass, the hydrodynamic volume of this series of polymer is different compared to the hydrodynamic volume of the reference.

3.5   THS measurements

Recently, research is being conducted into the possibility of using conjugated polymers in optical applications. The organic chromophores are particularly fascinating candidates for elaboration of optimized NLO materials because of their important chemical flexibility, easy, and low-priced preparation.[5] The use of polymers would allow a decrease in weight, size and cost of the applications. In this work, the TONO behavior of a series of P3AT is studied using the innovative THS technique. So, the optical behavior of different series of polythiophenes was studied, using three different types of measurements (static solvatochromism experiment, concentration series experiment and dynamic solvatochromism experiment). All these measurements were conducted using a tuneable Spectra-Physics Insight DeepSee femtosecond pulsed laser, as a high-power light source.

The polymers were placed in a standard quartz cuvette with optical path length of 2 mm or 10 mm and the light was focused into the cuvette. All the measurements are done by performing solvatochromism experiments. The polymer is dissolved in a good solvent (chloroform, $CHCl_3$) and a poor solvent (methanol, MeOH) is gradually added. Each sample and solvent used for the measurements had to be previously filtered to remove any unwanted solid residue which could interfere with the measurement.

As detector a Bruker Surespectrum 500 is spectrometer attached to an EMCCD Ixon 897 Andor camera was used. A representation of the setup is given in *Figure 9*.
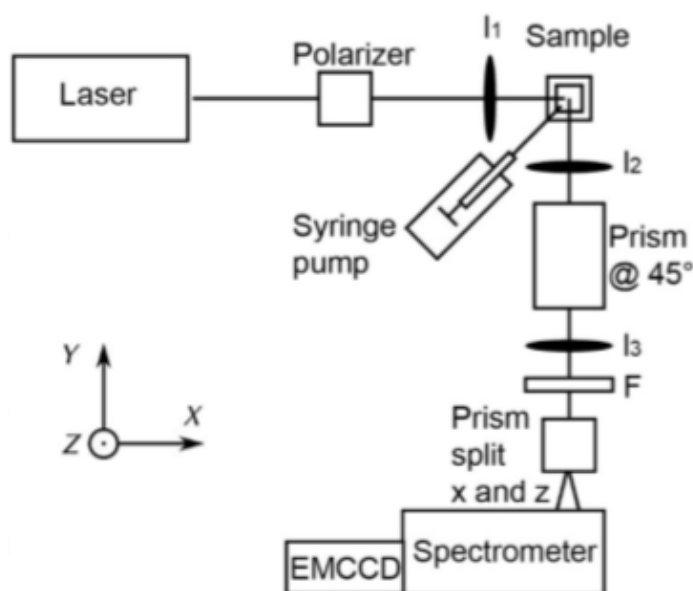
Figure 9. Laser configuration. Figure taken from article: Harmonic light scattering study reveals structured clusters upon the supramolecular aggregation of regio-regular poly(3-alkylthiophene); Michèle Moris et al. [6]

3.5.1 Static solvatochromism experiment

Via static solvatochromism experiments it was possible to study the aggregation behavior of the three series of polymers.

In a solvatochromism experiment, the polymers were dissolved in a good solvent ($CHCl_3$) and MeOH was gradually added in different steps using an automatic syringe (500 rpm, 0.25 mL/min).

In this way and by using the same conditions, the experiment is reproducible. The measurements were carried out until the polymer started to precipitate, because the polymers need to be in solution for having no interference with the laser beam. UV-vis measurements were also performed to study the aggregation behavior.[7] The amount of polymer used for this measurement was around 0.6 mg dissolved in 1 mL of $CHCl_3$. A part of the volume (0.1 mL) was taken and diluted again with 1 mL of $CHCl_3$. For these measurements a quartz cuvette with optical path length of 2 mm was used. The intensity of the incident laser beam (I_ω) was at 1300 nm (λ) which implies detection of the THS signal ($I_{3\omega}$) at 433 nm ($\lambda/3$).[8] $CHCl_3$ was used as an internal calibration standard, making it possible to correct the intensity of the polymer peaks for the contribution of the solvent. Every measurement was performed three times and an average of the obtained values was taken. To compare the different polymers with each other, it is important that the integration time is the same for each polymer, which is 5s in this case. The obtained values were plotted against wavelength as it is possible to see in the followed graphs, (*Figure 10-18 for P3HT series; Figure 19-27 for P3EHT series; Figure 28-32 for regio-isomers of P3HT series*).
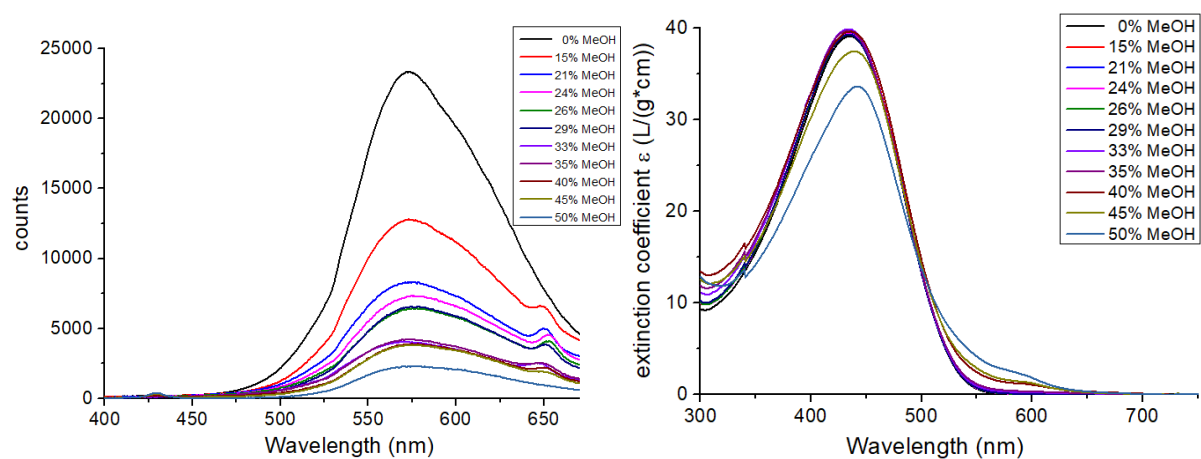
P3HT series

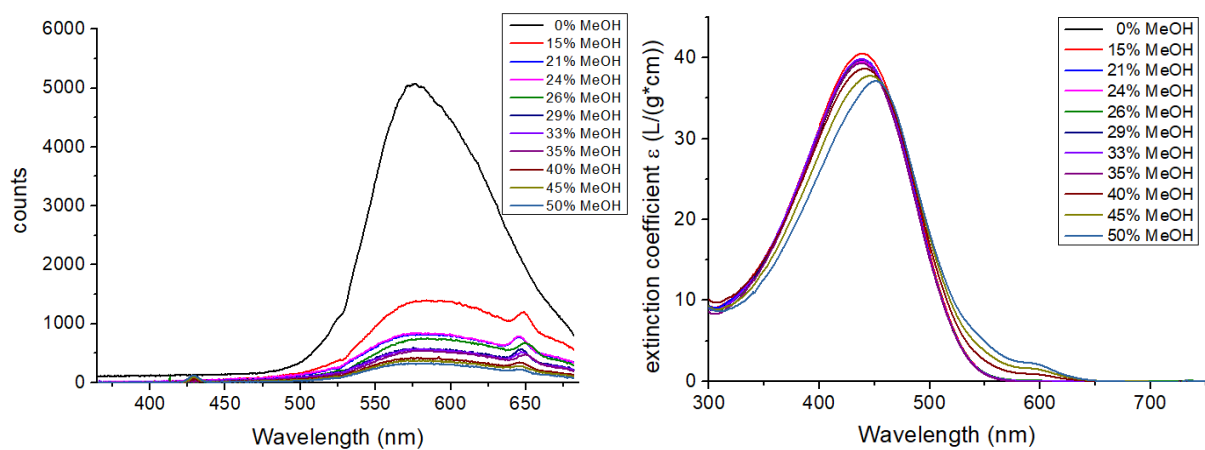*Figure 10. THS (left) UV-Vis (right) of P3HT with DP_13.*

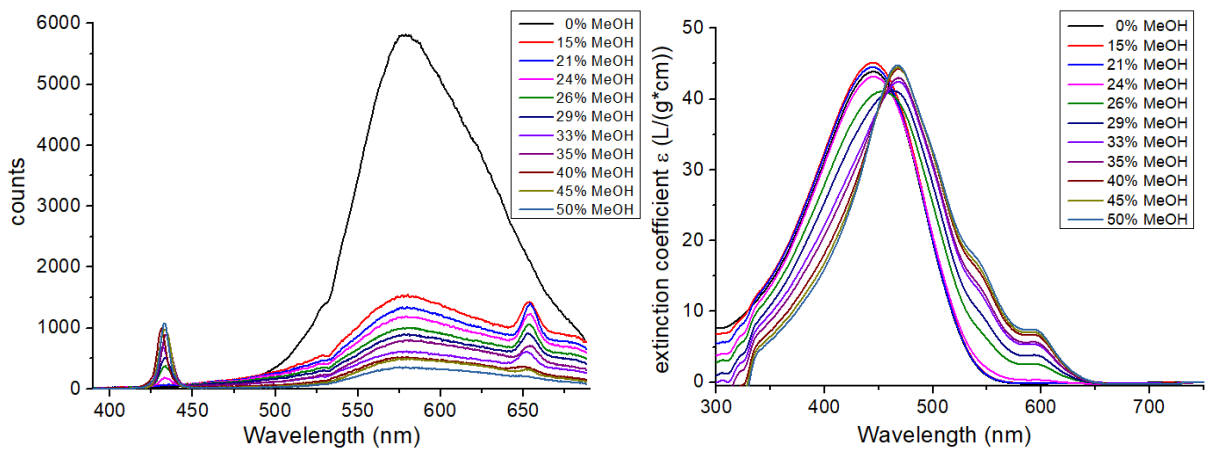*Figure 11. THS (left) UV-Vis (right) of P3HT with DP_15.*

Figure 12. THS (left) UV-Vis (right) of P3HT with DP_24.
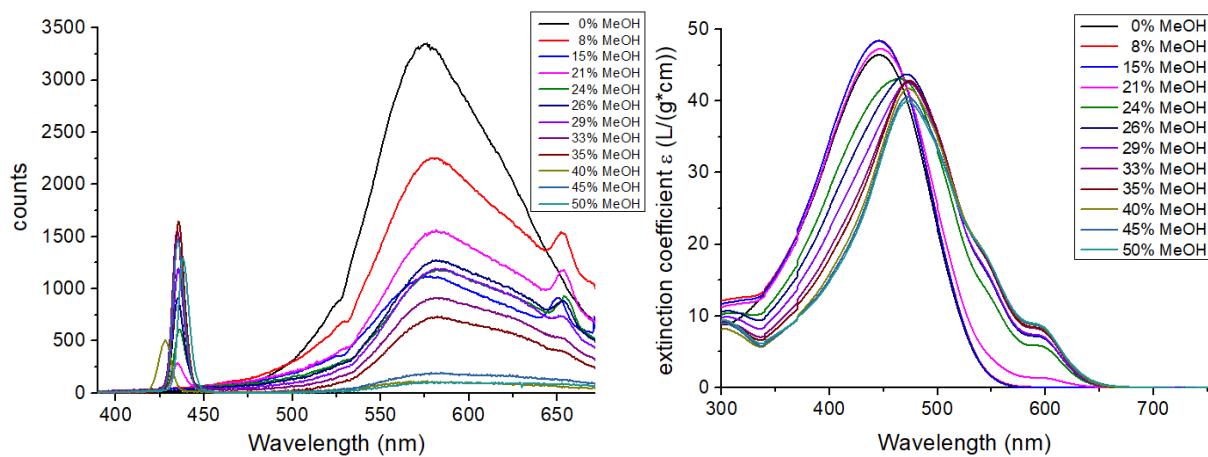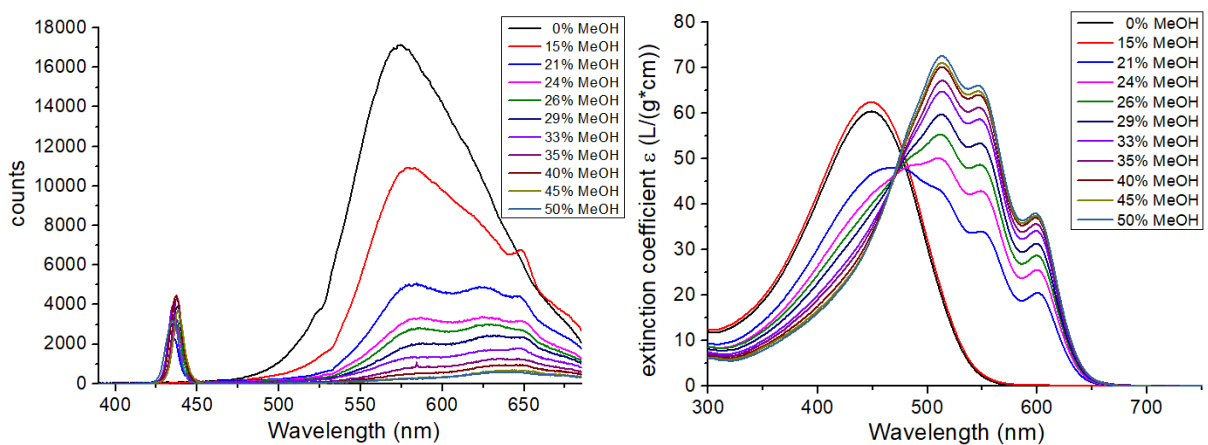
Figure 13.THS (left) UV-Vis (right) of P3HT with DP_28.

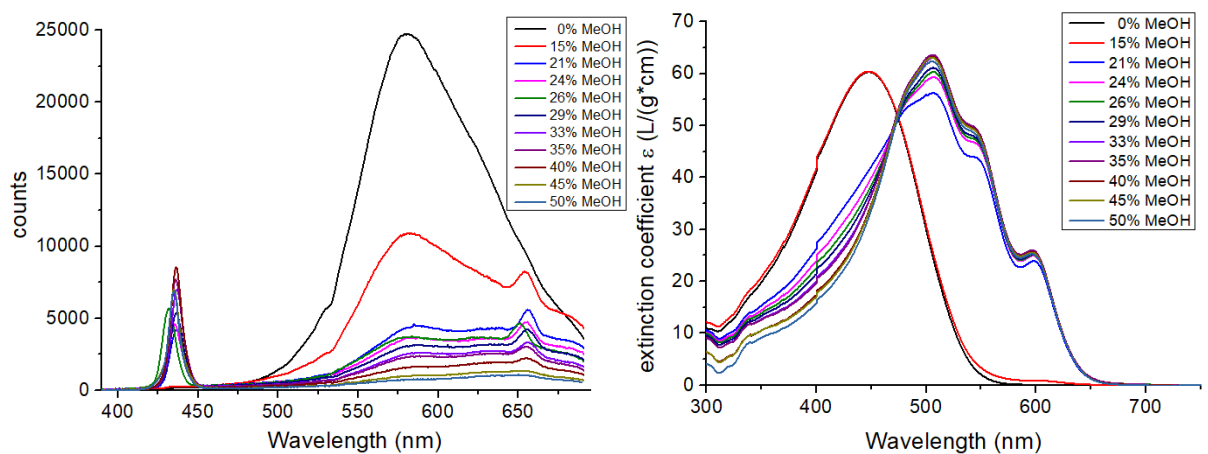
Figure 14.THS (left) UV-Vis (right) of P3HT with DP_37.

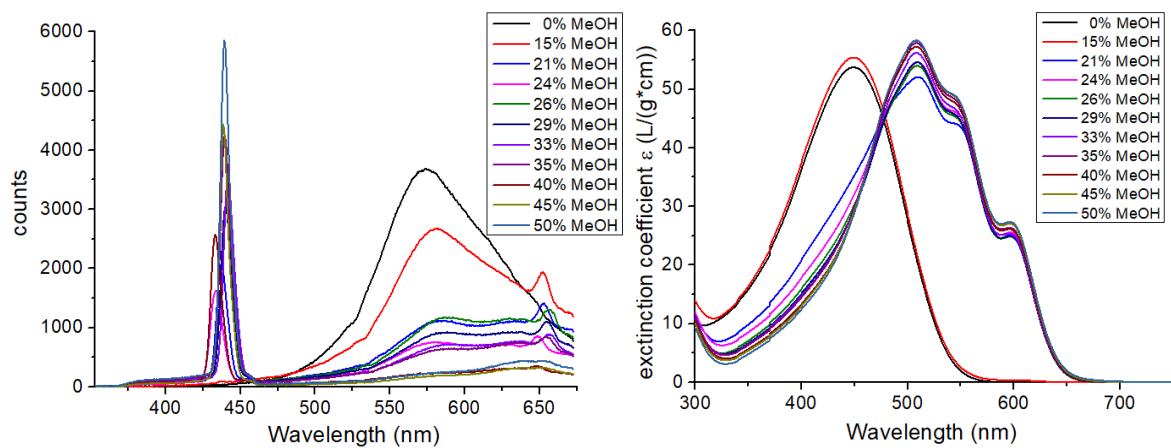*Figure 15. THS (left) UV-Vis (right) of P3HT with DP_41.*

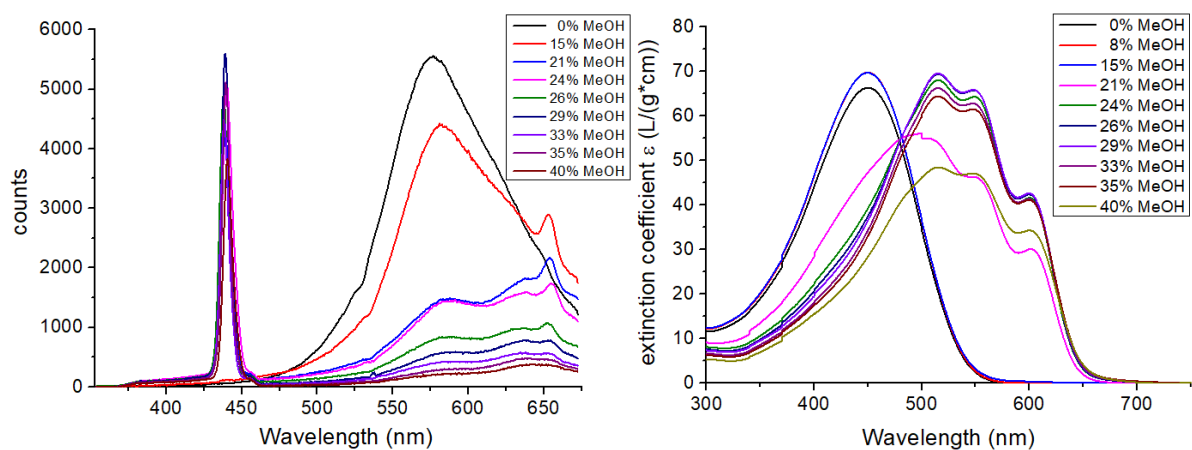*Figure 16.THS (left) UV-Vis (right) of P3HT with DP_45.*

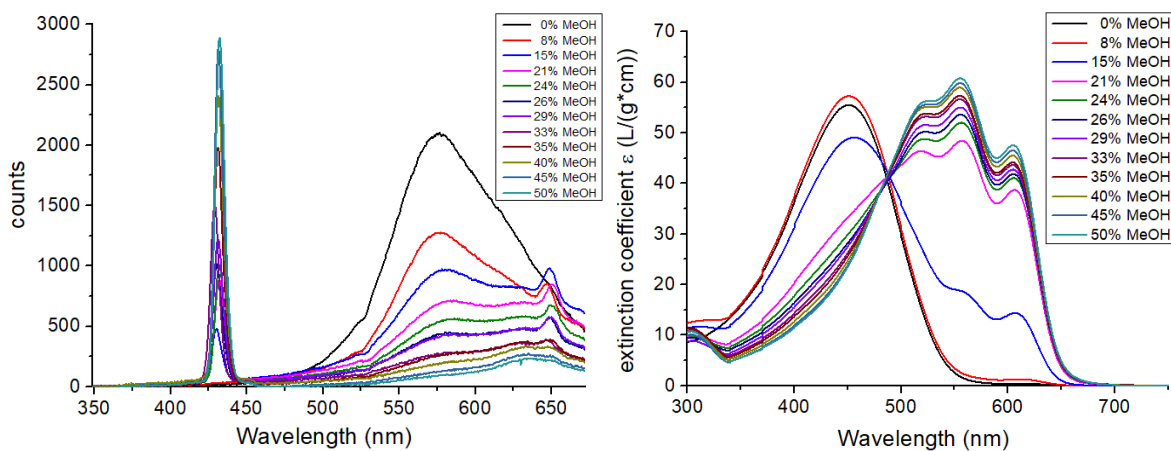*Figure 17. THS (left) UV-Vis (right) of P3HT with DP_55.*

Figure 18.THS (left) UV-Vis (right) of P3HT with DP_70.

It is possible to divide the harmonic scattering light graphs in three zones in function of the wavelength and the percentages of MeOH added: the third harmonic scattering peak, corresponding for the γ-value is visible at 433 nm. At 650 nm, the second harmonic scattering peak arises and in between (460 nm- 630 nm), the peak corresponds to the multiphoton induced fluorescence peak. The attention is focused on the intensity of the THS signal which is clearly increased with the increase of the DP, in this series of P3HT.

UV-Vis spectroscopy provides information on compounds that have conjugated double bonds.

The highest-energy electronic transition π-π*, is related to the promotion of an electron from a binding molecular orbital to an anti-bonding molecular orbital. The wavelength (λ) relative to the highest value of the absorption band is λ_{max}. The absorption bands are wide since each electronic state has vibrational sublevels and electronic transitions can occur between different vibrational sublevels, consequently, electronic transitions can occur in a range of wavelengths. In the UV-Vis graphs (*Figure 10-18*) of the P3HT series it is seen that a red shift of λ_{max} is visible after the addition of around 21% of MeOH for almost all the polymers. For P3HT_DP13/15 there is a red shift of λ_{max} at higher percentages of MeOH but it is not that much pronounced as in the other polymers probably due to the less aggregation behavior of a polymer with a low DP. In order, it is clearly present a vibration fine structure around 600 nm which is more evident in polymers with high DP.
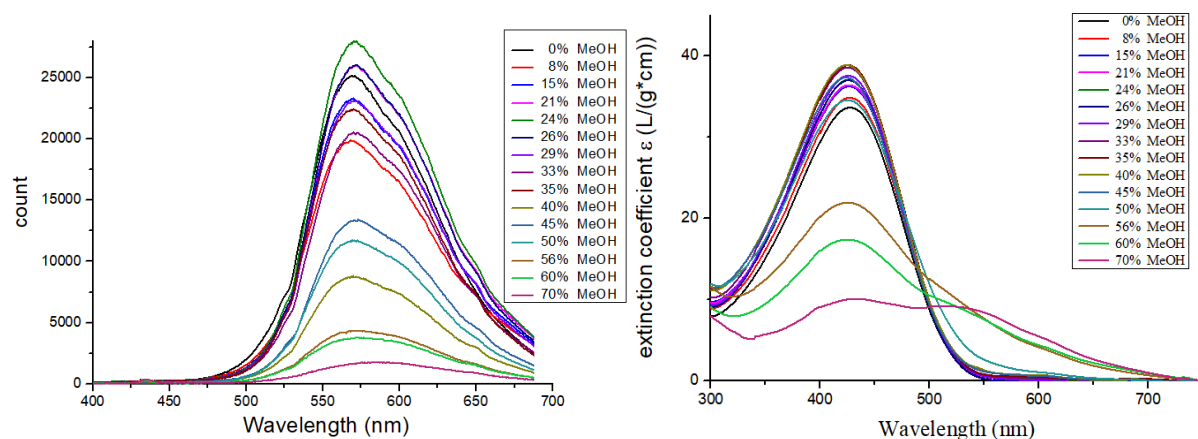
P3EHT series
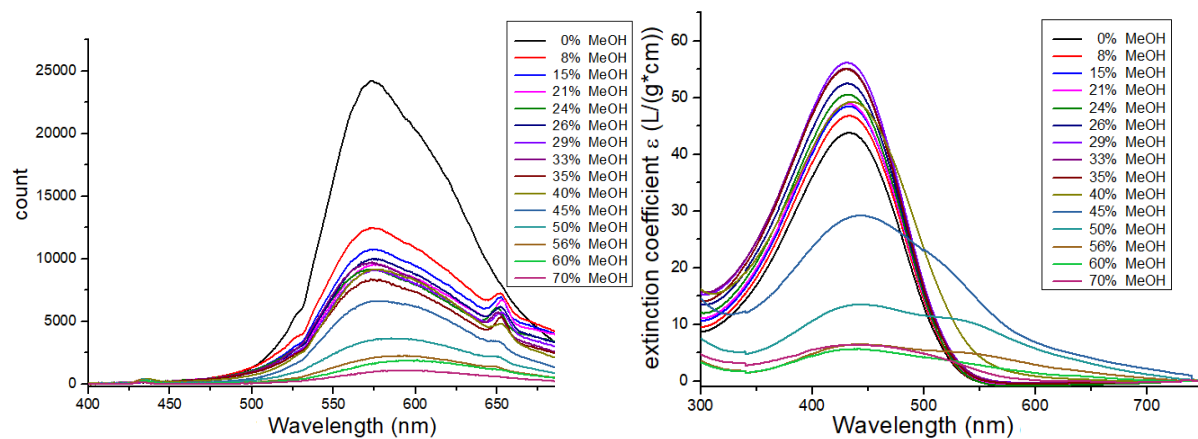

Figure 19. THS (left) UV-Vis (right) of P3HT with DP_18.

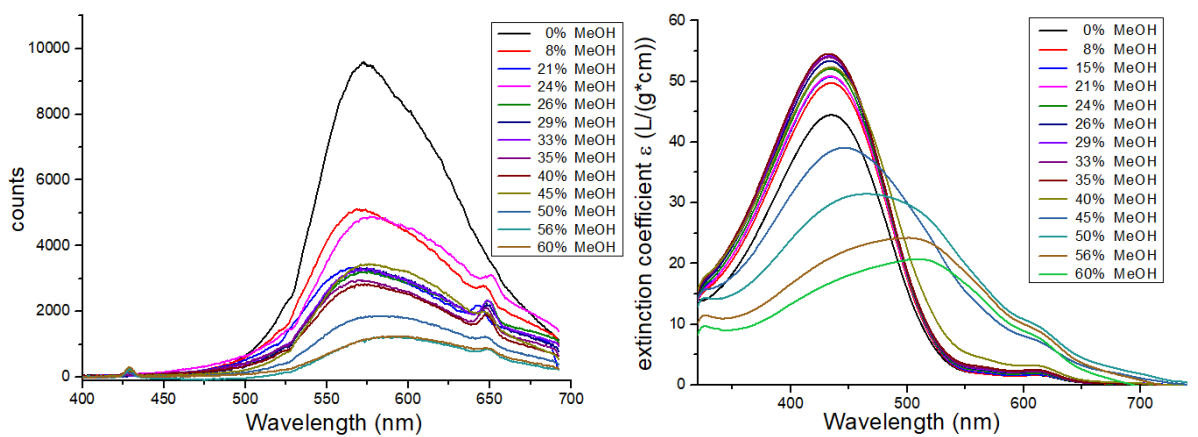*Figure 20. THS (left) UV-Vis (right) of P3HT with DP_23.*

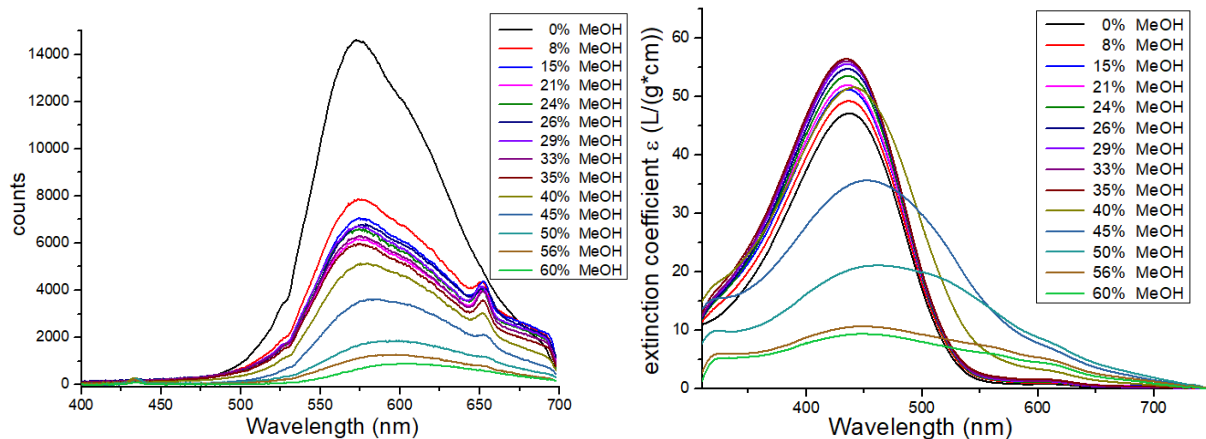*Figure 21. THS (left) UV-Vis (right) of P3HT with DP_29.*

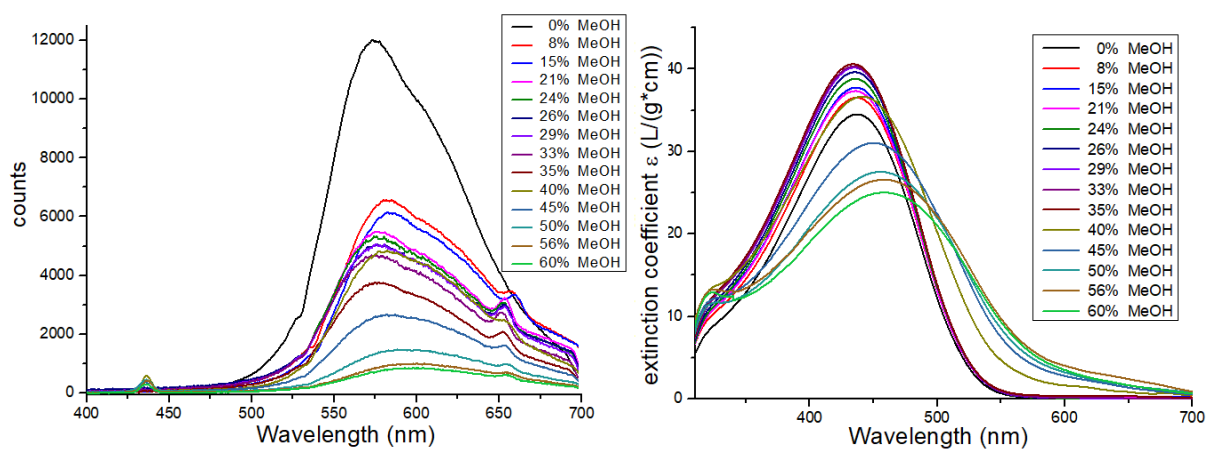*Figure 22. THS (left) UV-Vis (right) of P3HT with DP_39.*

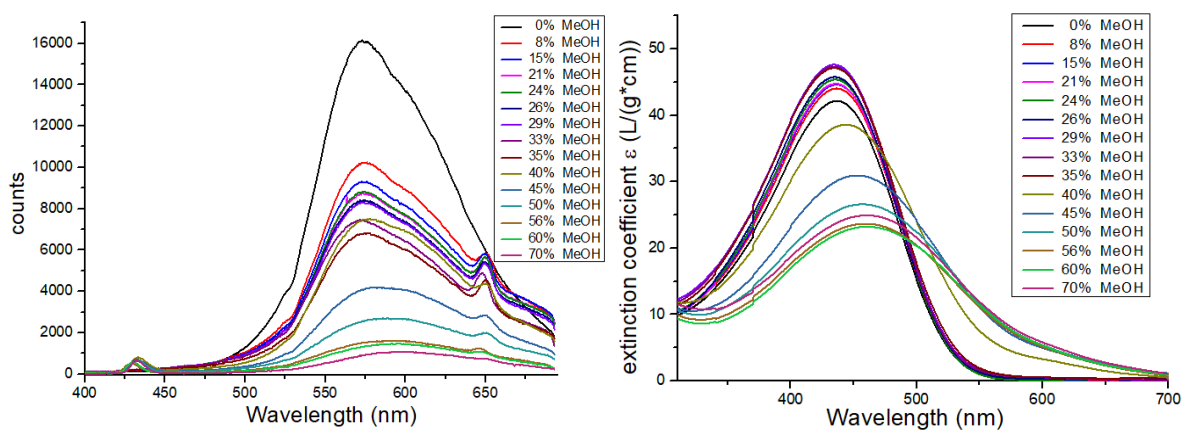*Figure 23. THS (left) UV-Vis (right) of P3HT with DP_45.*

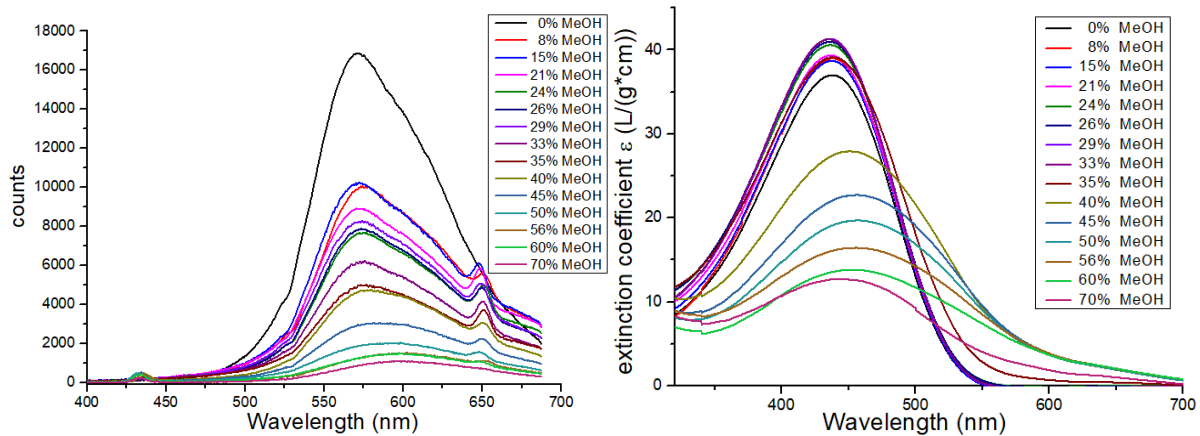*Figure 24. THS (left) UV-Vis (right) of P3HT with DP_48.*

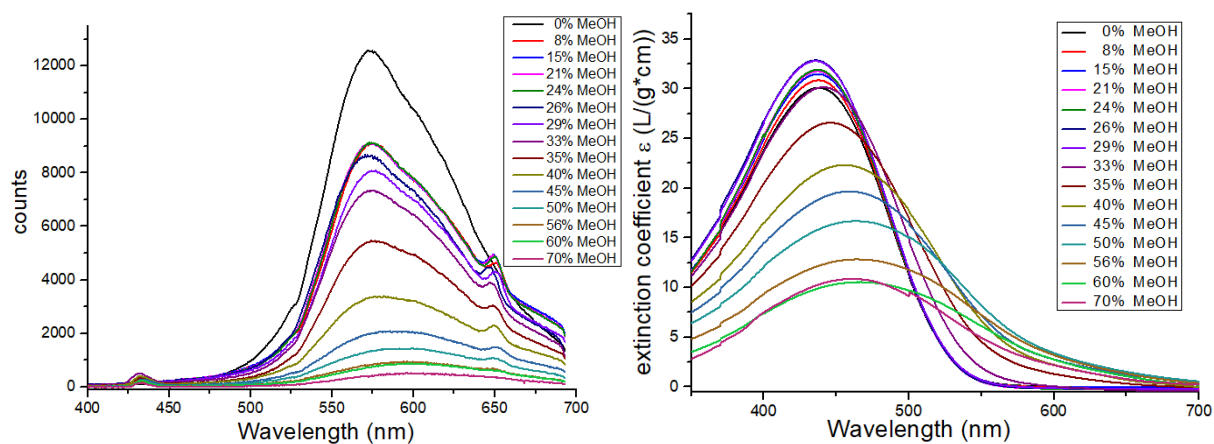*Figure 25. THS (left) UV-Vis (right) of P3HT with DP_60.*

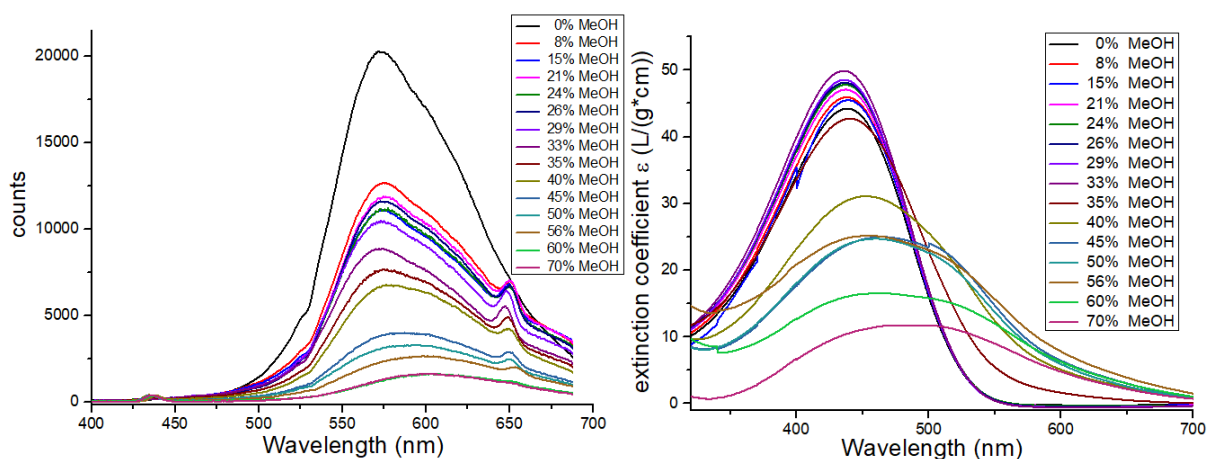*Figure 26. THS (left) UV-Vis (right) of P3HT with DP_71.*

Figure 27. THS (left) UV-Vis (right) of P3HT with DP_78.

As said before the harmonic scattering light graphs could be divided in three zones but the attention is focused on the intensity of the THS signal which is found at 433 nm. In this series of polymers there is not a clear trend as before. Indeed, there is not a real trend with the increase of the DP, the THS peaks is almost absent in polymers with a low DP(DP_18/23). From the P3EHT_DP_45 it is possible to see an increase of the THS signal but in general it could be said that the THS signal is almost constant in this series of polymers.

The trend of the P3EHT series could be associated to the less aggregation behavior of the polymers due to the high presence of steric hinderance given by the ethyl group.

The branching in the side chain has an influence on the π-π stacking of the P3EHT compare to the unbranched P3HT; the covalent bonding between the aromatic rings is less strong due to the steric hinderance and therefore the aggregation is more hampered.

In the UV-Vis graphs (*Figure 19-27*) it is seen that there is a red shift of λ_{max} for all the polymers which started after an addition of 40-45% of MeOH but it is more pronounced for the polymers with a high DP. Indeed, for the P3EHT series a vibrational fine structure around 600 nm is not present as it was clearly visible for the P3HT series. It is probably due to the fact that the branching of P3EHT involve in a less well-organized structure compare to the P3HT structure.

Regio-isomer P3HT series
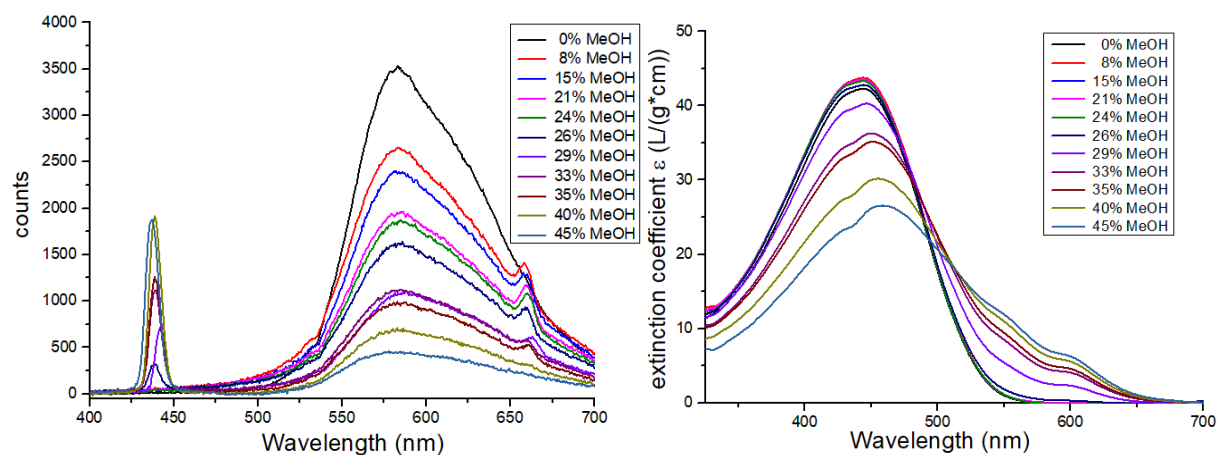
Figure 28. THS (left) UV-Vis (right) of regio.isomers of P3HT of P1.
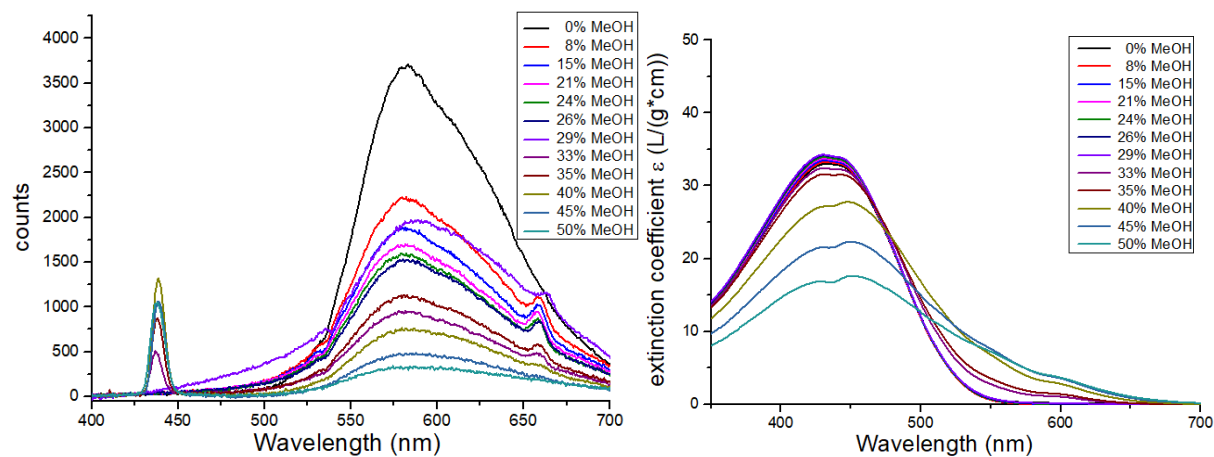
Figure 29. THS (left) UV-Vis (right) of regio.isomers of P3HT of P2.
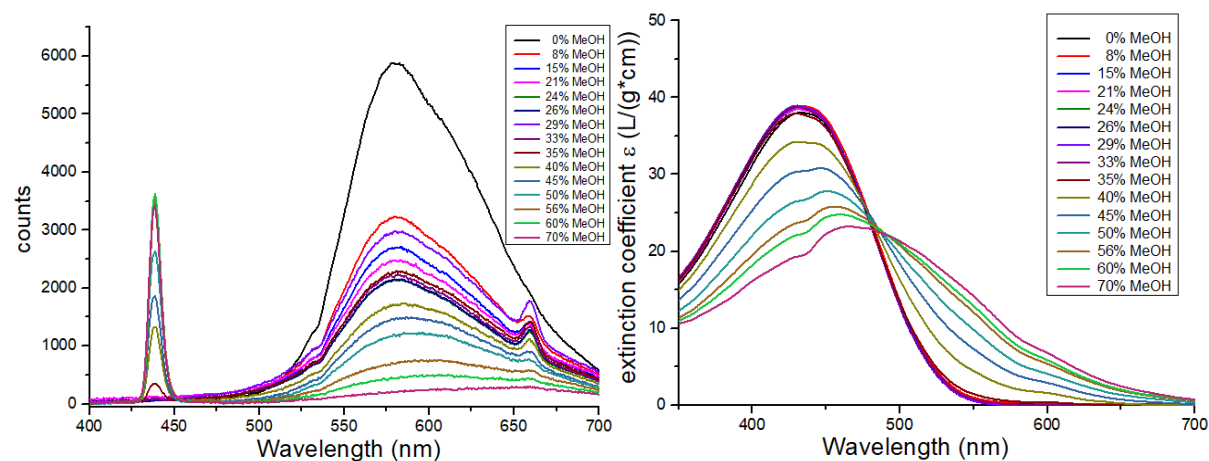
Figure 30. THS (left) UV-Vis (right) of regio.isomers of P3HT of P3.
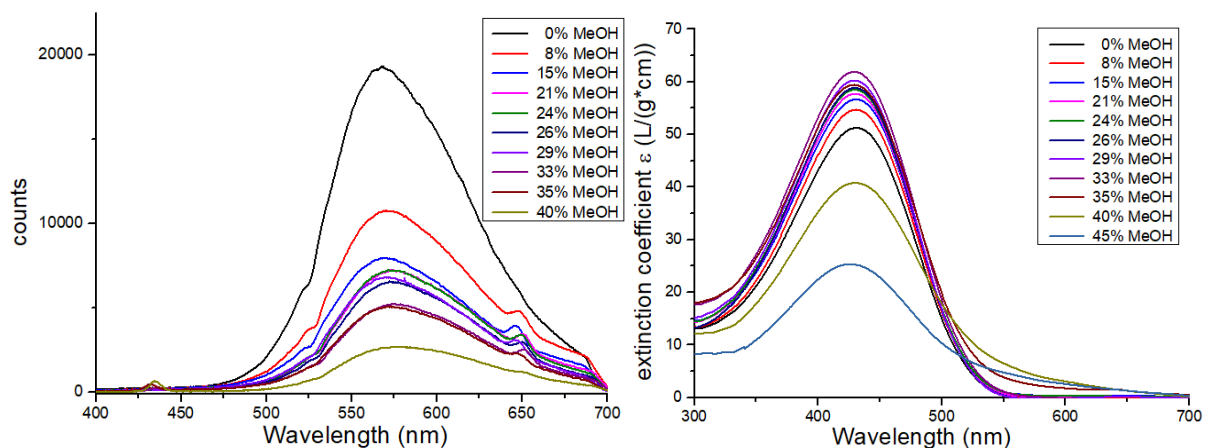
Figure 31. THS (left) UV-Vis (right) of regio.isomers of P3HT of P4.
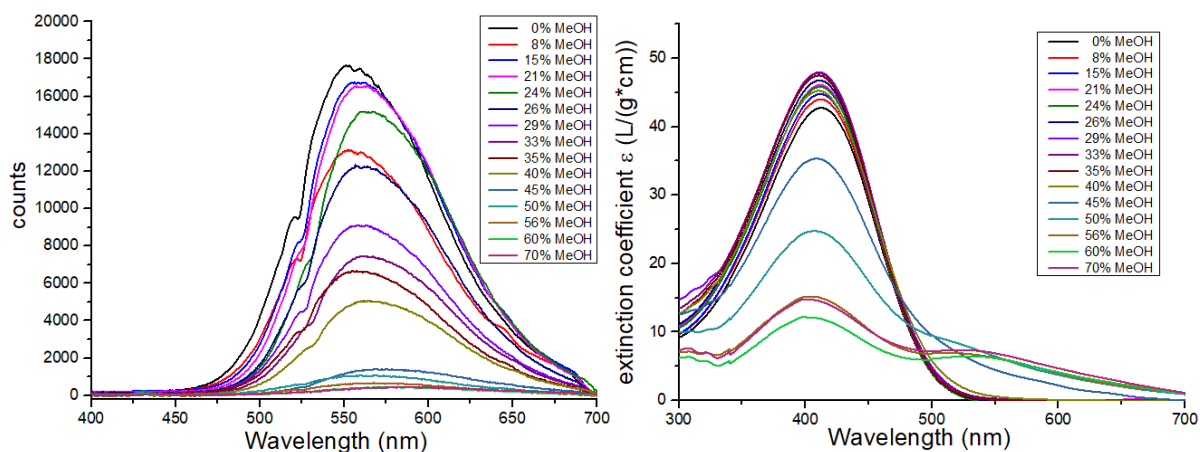
Figure 32. THS (left) UV-Vis (right) of regio.isomers of P3HT of P5.

For the last series of polymers, the attention is focused on the trend of the THS signal in function of different regio-regularities of the polymers. As it is showed in the sequence of graphs it is clear that the THS signal decreased with the increase of the regio-irregularity. In the UV-Vis graphs (*Figure 28-32*) it is seen that a red shift of λ_{max} is visible for P1, P2 and P3 after the addition of around 29% of MeOH and a vibrational fine structure is as well present. For P4 and P5 there is a red shift of λ_{max} but there is not a clear vibrational fine structure around

600 nm present probably due to the less aggregation behavior of a polymer with a high regio-irregularity.

3.5.2 Concentration experiment

Via concentration series experiments it was possible to study the γ-value of the three series of polymers. In a concentration experiment, the polymers were dissolved in a good solvent ($CHCl_3$) and MeOH was gradually added in different steps using an automatic syringe (500 rpm, 0.25 mL/min). In this way and by using the same conditions, the experiment is reproducible.

The volume of MeOH added was different for each polymer and depends on the maximum value of THS peak which was obtained from the static solvatochromism experiments.

The amount of polymer used for this measurement was around 0.6 mg dissolved in 1 mL of $CHCl_3$. A part of that volume (0.1 mL) was taken and diluted again with 1 mL of $CHCl_3$. For these measurements a quartz cuvette with optical path length of 10 mm was used. The intensity of the incident laser beam was at 1300 nm (λ) and the intensity of the THS signal was detected at 433 nm ($\lambda/3$).

Trans-stilbene (TS) was used as reference, since its γ-value is already known from precedent studies.[8] For the P3HT series, $CHCl_3$ was as well used as a reference. But since it is very hard to see the solvent signal, it is not further used for the measurements of P3EHT and P1-P5.

In this concentration series experiment, for each polymer, 0.250 mL of MeOH was added seven times during the analysis and after each addition 5 measurements were performed. The measurements were performed in a way to isolate the peak of the THS signal at $\lambda/3$ = 433 nm, in particular, from the multiphoton induced fluorescence.

The obtained THS peak was fitted using a Gaussian fit function to determine the area under the THS peak. Afterward, the obtained area's in function of the concentration were plotted. By using a linear fit, the slope of the curve can be

determinated, necessary to obtain the γ-value. The γ-value can then be calculated using next formula:

$$\gamma = \sqrt{\left(\gamma_{,TS}\right)^2 * \frac{Slope}{Slope_{TS}} * correction\ factor}$$

The correction factor is correlated to the refractive index (n) of the sample.

In the followed graphs the γ-value in function of the DP or the polymers itself are plotted. As already said before, for the P3HT series the γ-value was calculated using both of the references (CHCl$_3$ and TS), for the other two series it was only measured against TS.

In *Figure 33*, the values obtained from the two references are quite similar except for P3HT_DP_70 and there is clearly a trend: the γ-value increases with the DP.

For P3EHT series as shown in *Figure 34*, there is not a real trend as it was said for the static solvatochromism experiment, in fact, it seems more like the γ-value is a constant.

In the last series of polymers, in *Figure 35*, the γ-value decreases with the increase of the regio-irregularity.
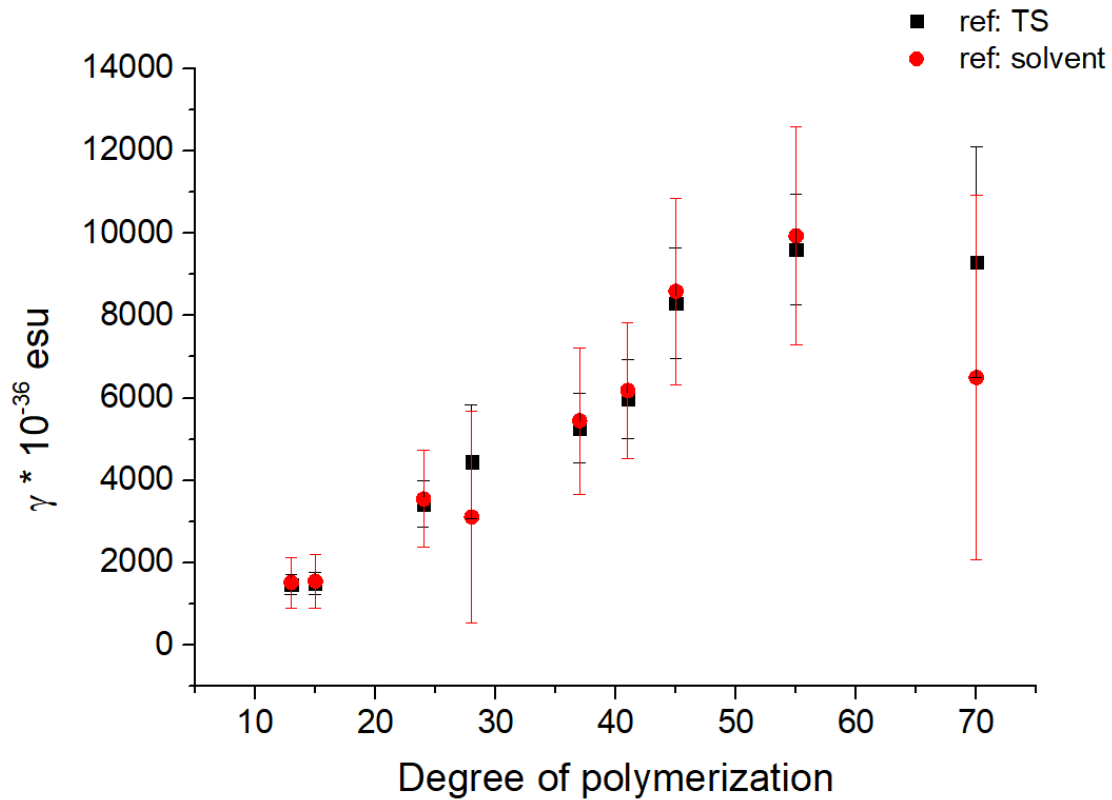
Figure 33. γ-value P3HT series.
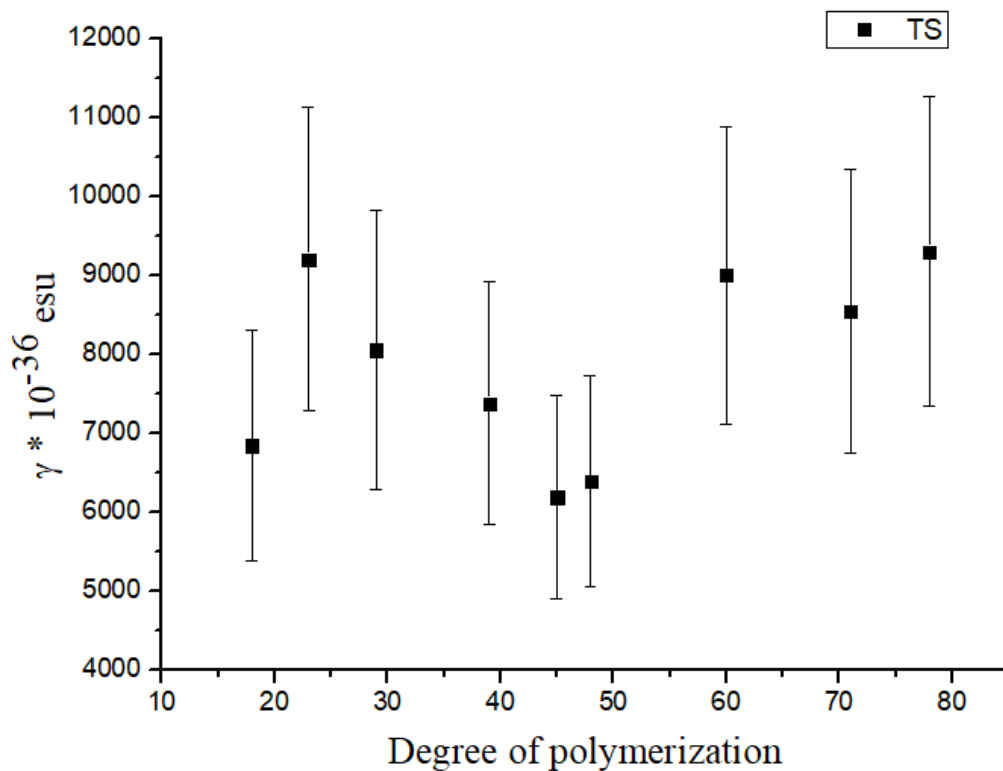
Figure 34. γ-value P3EHT series.
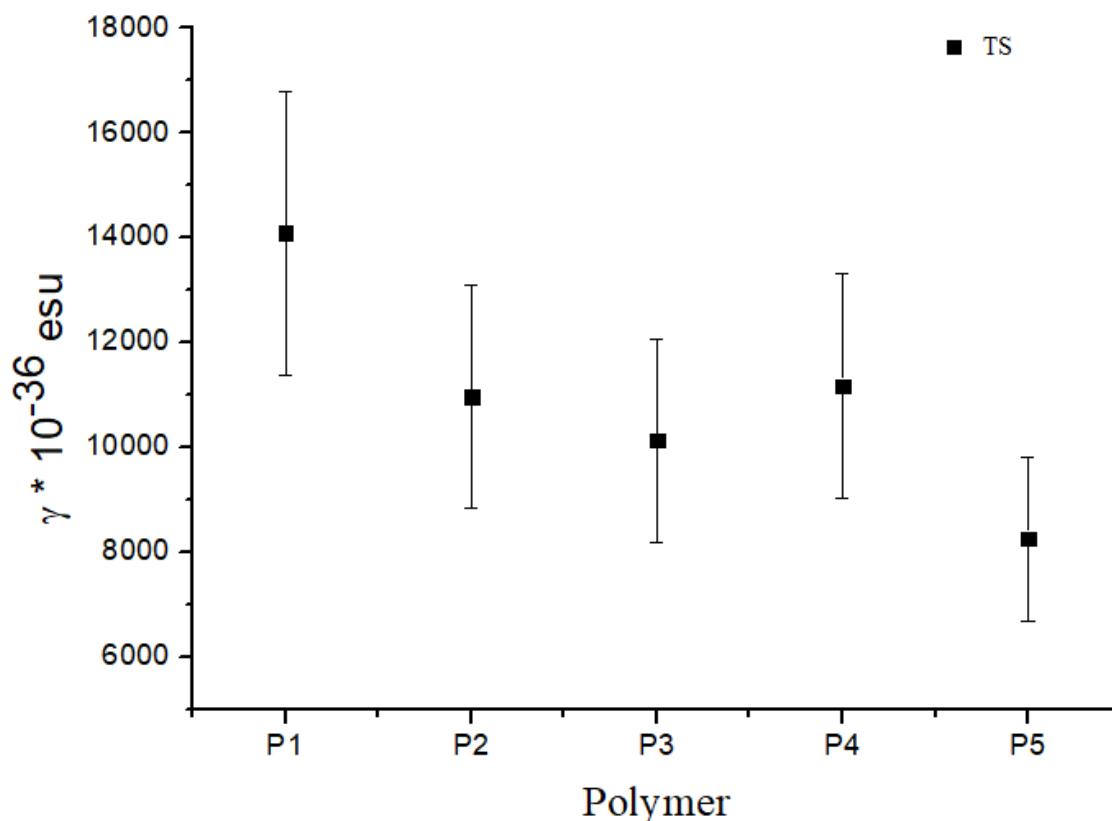
Figure 35. γ-value P3HT regio-isomer series.

3.5.3 Dynamic solvatochromism experiment

Via dynamic solvatochromism experiments it was possible to study the aggregation behavior of the three series of polymers, in a determinated data acquisition time. In a dynamic solvatochromism experiment, the polymers were dissolved in a good solvent ($CHCl_3$) and MeOH (1.6 mL) was gradually added using an automatic syringe (500 rpm, 0.25 mL/min) while the solution was stirred. In this way and by using the same conditions, the experiment is reproducible. The amount of polymer used for this measurement was around 0.6 mg dissolved in 1 mL of $CHCl_3$. A part of that volume (0.1 mL) was taken and diluted again with 1 mL of $CHCl_3$. For these measurements, a quartz cuvette with optical path length of 10 mm was used. The intensity of the incident laser beam (was at 1300 nm (λ) and the intensity of the THS signal) was detected at 433 nm ($\lambda/_3$).

In the dynamic solvatochromism experiment, the obtained area of the THS peak is plotted in function of the percentage of MeOH added. As we can see in *Figure 36*, the aggregation of P3HT_DP55/45 started earlier compare to the other polymers. There is a general trend by which the polymer with a higher DP start to aggregate earlier compared to the polymer with a low DP (P3HT_DP_13/15). There is the same trend for the P3EHT series (*Figure 37*).

Moreover, for the regio-regularity P3HT series it is seen that the polymers with a high regio-regularity started to aggregate earlier than the others, as shown in *Figure 38*.

Figure 36. Dynamic solvatochromism of P3HT.

Figure 37. Dynamic solvatochromism of P3EHT.
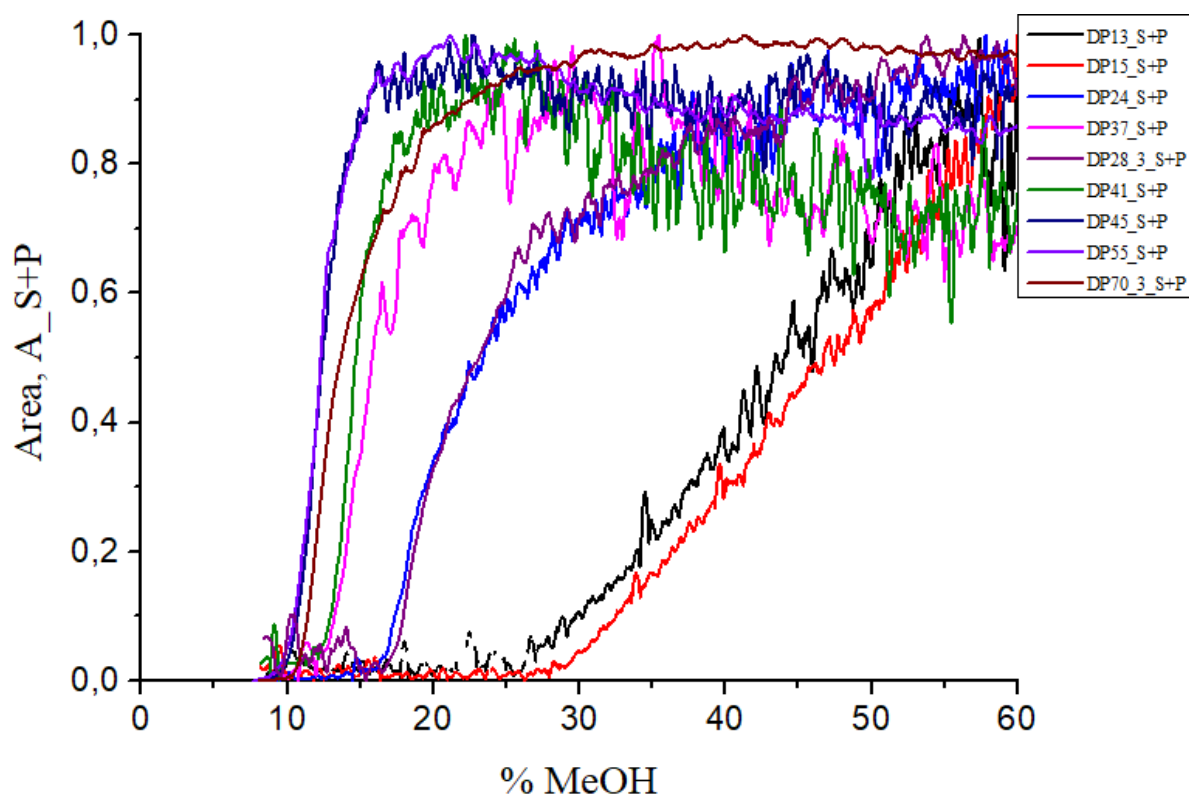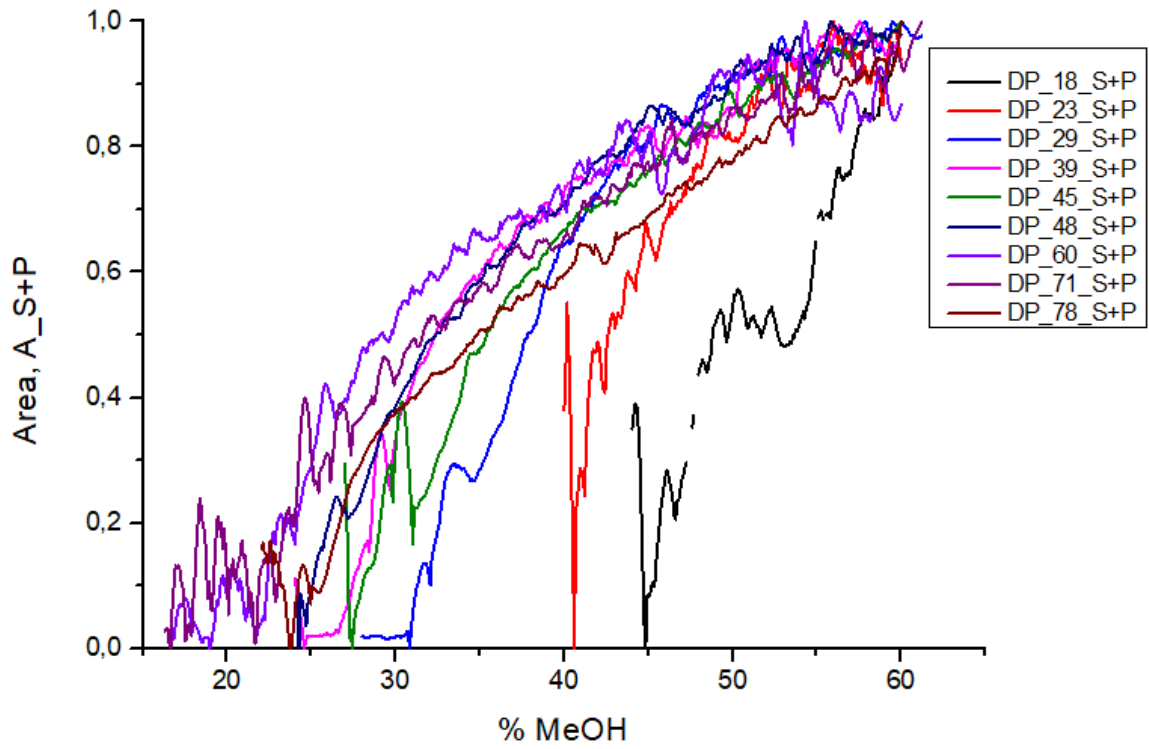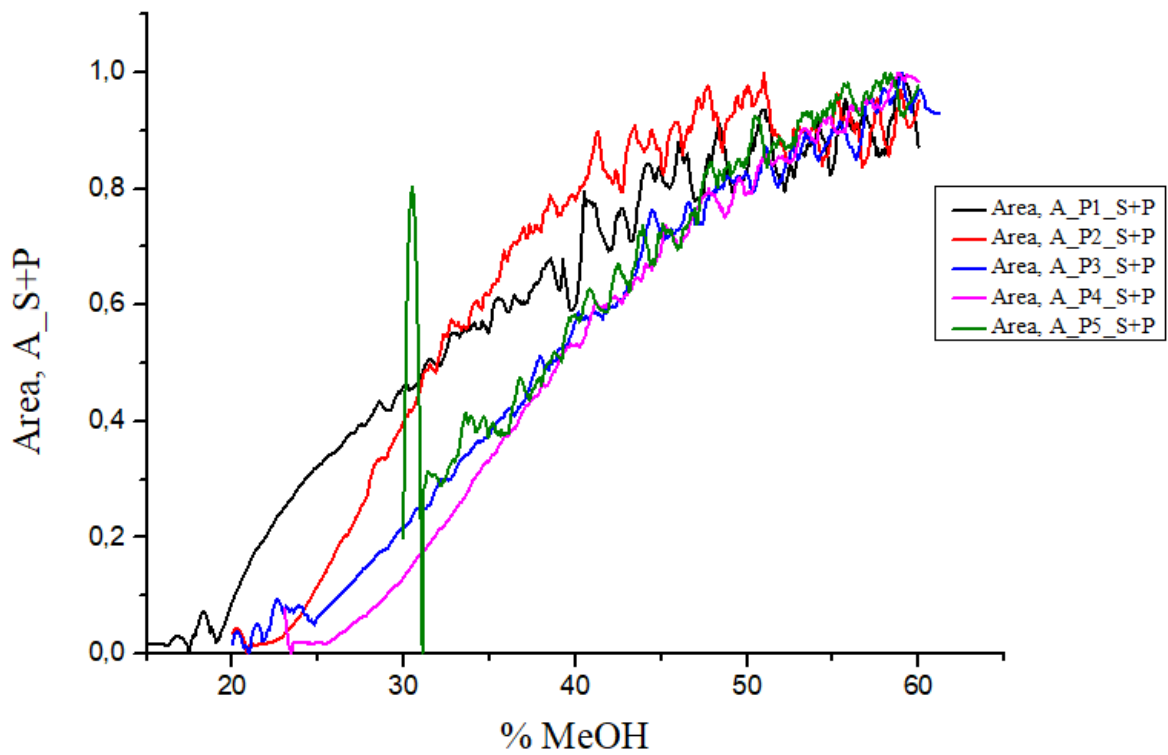

Figure 38. Dynamic solvatochromism of regio-isomers of P3HT.

Bibliography of Chapter 3

1. Lize Verheyen, Pieter Leysen, Marie-Paule Van Den Eede, Ward Ceunen, Tine Hardeman, Guy Koeckelberghs; Advances in the controlled polymerization of conjugated polymers; Polymer, 108, 521-546, (2017).

2. Han, J., Yin, H., Liu, C., Wang, J. & Jian, X. Construction of donor-acceptor polymers containing thiophene-phthalazinone moiety via classic Ullmann C[sbnd]N coupling polymerization and their optical-electrical properties. Polym. (United Kingdom) 101, 241–256, (2016).

3. Alfons Smeets, Karlien Van den Bergh, Julien De Winter, Pascal Gerbaux, Thierry Verbiest, and Guy Koeckelberghs; Incorporation of Different End Groups in Conjugated Polymers Using Functional Nickel Initiators; Macromolecules, 42, 7638–7641, (2009).

4. Giovanna Barbarella, Alessandro Bonghi, and Massimo Zambianchi; Regiochemistry and Conformation of Poly-3-hexylthiophene) via the Synthesis and the Spectroscopic Characterization of the Model Configurational Triads, Macromolecules; 27,3039-3045, (1994).

5. Pieter Willot, Joost Steverlynck, David Moerman, Philippe Lecle`re, Roberto Lazzaroni and Guy Koeckelberghs; Poly(3-alkylthiophene) with tuneable regioregularity: synthesis and self-assembling properties; Polym. Chem.; 4, 2662, (2013).

6. Michèle Moris; Marie-Paule Van Den Eede, Guy Koeckelberghs, Olivier Deschaume, Carmen Bartic, Stijn Van Cleuvenbergen, Koen Clays & Thierry Verbiest; Harmonic light scattering study reveals structured clusters upon the supramolecular aggregation of regioregular poly(3-alkylthiophene); Communications Chemistry, 130, (2019).

7. Benedetta Carlotti, Alessio Cesaretti, Oliviero Cannelli, Tommaso Giovannini, Chiara Cappelli, Carmela Bonaccorso, Cosimo G. Fortuna, Fausto Elisei and Anna Spalletti.; Evaluation of Hyperpolarizability from the Solvatochromic Method: Thiophene Containing Push−Pull Cationic Dyes as a Case Study; J. Phys. Chem. C, 122, 2285-2296, (2018).

8. Nick Van Steerteghem, Koen Clays, Thierry Verbiest, and Stijn Van Cleuvenbergen; Third-Harmonic Scattering for Fast and Sensitive Screening of the Second Hyperpolarizability in Solution; Anal. Chem.; 89, 2964−2971, (2017).

CHAPTER 4: CONCLUSION

The aim of the presented project was to verify the possibility to put a first step in the performance of TONO materials by investigating several parameters of three different series of P3AT. In particular, the attention was focused on the investigation of the γ-value using a recent THS technique.

This project started by investigating the influence of the molar mass on the γ-value. Therefore, a series of P3HT with different DP was synthesized using KCTCP. The difference in molar mass was confirmed by GPC and ^{1}H-NMR. Afterward, the polymers were studied by UV-vis and THS measurements. Out of these results, it can be concluded that for P3HT the γ-value increases with the DP.

After that another series of P3EHT, with different DP, was synthesized as well by KCTCP. The branching in the side chain has an influence on the π-π stacking of the P3EHT compare to the unbranched P3HT; the covalent bonding between the aromatic rings is less strong due to the steric hinderance of the side chain and therefore the aggregation is more hampered. This all have an influence on the charge transfer within the polymer backbones. This is seen in the THS measurements were the γ-value for this series of polymers is more a constant compared to P3HT where there is an influence of the DP.

In the last part of this project the influence of regioregularity on the γ-value was also investigated. Therefore, a series of a random copolymer, with a defined DP, of the two regio-isomers of P3HT was synthesized by varying the ratio of the two regio-isomers. The γ-value decreases with the increase of the regio-irregularity. The organization of P3HT depends on the amount of regio-regularity which have as well an influence on the charge transport.

In conclusion, the presented research project showed that it is possible to obtain positive feedback from measuring the γ-value for the three series of different P3AT. It is also proven that the branching and regio-regularity have an important influence on the γ-

value. The more the aggregation behaviour is hampered, which implies a less charge transport, the lower the γ-value is.

CHAPTER 5: EXPERIMENTAL PART
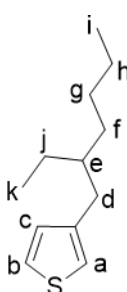
5.1 Synthesis of the precursor monomer 2-bromo-3-(2-ethylhexyl)-5-iodothiophene

5.1.1 Synthesis of 3-(2-ethylhexyl)thiophene

A nitrogen purged solution of 1-bromo-2-ethylhexane (19.33 g, 100 mmol) in dry Et_2O was added slowly to a stirred solution of Mg turnings (2.43 g, 100 mmol) in 20 mL of dry Et_2O. After 2 hours of refluxing, the solution was cooled to 0 °C. After which it was cannulated to a nitrogen purged solution of $Ni(dppp)Cl_2$ (0.54 g; 1.00 mmol) and 3-bromothiophene (16.07 g; 98 mmol) in dry Et_2O (25 mL). After 3 hours of refluxing, the reaction was quenched by slowly pouring out the solution into an ice-cold 1 M HCl solution. The formed precipitate was filtered off and subsequently the filtrate was extracted with Et_2O. Afterward, the organic layers were successively washed with a saturated $NaHCO_3$- and NaCl-solution. The organic layer was dried using $MgSO_4$, filtered off and the solvent was removed under reduced pressure. After purification by vacuum distillation and column chromatography (SiO_2, eluent: heptane) a colourless oil was obtained as pure product. (11.13 g; 56.70 mmol).

Final amount: 11.13 g

Y= 57%
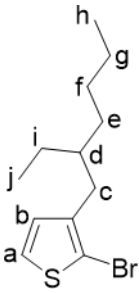
^{1}H-NMR (CDCl$_3$)	δ (ppm)	#H (mp; J)	H$_?$
	7.22	1 (dd; J = 1.8 Hz; J = 2.4 Hz)	b
	6.90	2 (m)	a, c
	2.56	2 (d)	d
	1.26	9 (m)	e, f, g, h, j
	0.87	6 (m)	i, k

5.1.2 Synthesis of 2-bromo-3-(2-ethylhexyl)thiophene

A solution of 3-(2-ethylhexyl) thiophene (11.13 g; 56.70 mmol) in THF (250 mL) was shielded from light and placed under nitrogen atmosphere at 0°C. NBS (8.58 g; 48.2 mmol) was added in small quantities to the stirred solution. The reaction was stirred at room temperature for one night and followed up by ^{1}H-NMR. After completion of the reaction, the reaction mixture was quenched with $Na_2S_2O_3$ and extracted with heptane. The organic layer was successively washed with a saturated NaOH-, $NaHCO_3$-, and NaCl-solution. The organic layer was dried using $MgSO_4$, filtered off and the solvent was removed under reduced pressure. Purification by chromatography column (SiO_2, eluent: heptane) produced a colourless oil (5,705 g, 20,7 mmol), of which the purity was confirmed via ^{1}H-NMR.

Final amount: 5,705 g

Y= 37%

^{1}H-NMR (CDCl$_3$)	δ (ppm)	#H (mp)	H?
	7.18	1 (d)	b
	6.76	1 (d)	a
	2.50	2 (d)	c
	1.28	9 (m)	d, e, f, g, i
	0.88	6 (m)	h, j

5.1.3 Synthesis of 2-bromo-3-(2-ethylhexyl)-5-iodothiophene
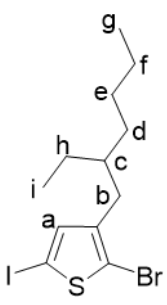
A solution of 2-bromo-3-(2-ethylhexyl)thiophene (5.705 g; 20.7 mmol) in DCM (150 mL) was placed under nitrogen atmosphere, shielded from light and brought to 0 °C. After addition of (diacetoxyiodo)benzene (3.33 g; 10.35 mmol) to the stirred solution, I_2 (2.63 g; 10.35 mmol) was gradually added. After overnight stirring at room temperature, the conversion rate was determined via ^{1}H-NMR. The reaction was quenched with $Na_2S_2O_3$. After extraction with heptane, the organic layer was successively washed with a saturated $NaHCO_3$-, and NaCl-solution. The organic layer was dried using $MgSO_4$, filtered off and the solvent was removed under reduced pressure. After removal of the solvent, the formed secondary product, iodine benzene, was removed using a vacuum distillation. After purification via column chromatography (SiO_2, eluent: heptane) a pale-yellow oil was obtained (6.94 g; 17.30 mmol). The purity was checked with ^{1}H-NMR.

Final amount: 6,94 g

Y= 84%

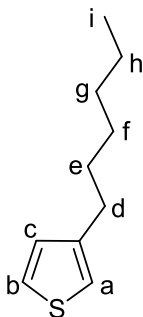| ^{1}H-NMR (CDCl$_3$)	δ (ppm)	#H (mp)	H$_?$
	6.93	1 (s)	a
	2.46	2 (d)	b
	1.28	9 (m)	c, d, e, f, h
	0.88	6 (m)	g, i

5.2 Synthesis of the precursor monomer 5-bromo-3-hexyl-2-iodothiophene

5.2.1 Synthesis of 3-hexylthiophene

A nitrogen purged solution of 1-bromohexane (16.52 g; 100 mmol) in dry Et_2O was added slowly to a stirred solution of Mg turnings (2.44 g; 100 mmol) in 20 mL of dry Et_2O. After 2 hours of refluxing, the solution was cooled to 0 °C. After which it was cannulated to a nitrogen purged solution of $Ni(dppp)Cl_2$ (0.55 g; 1.00 mmol) and 3-bromothiophene (15.99 g; 98 mmol) in dry Et_2O (25 mL). After 3 hours of refluxing, the reaction was quenched by slowly pouring out the solution into an ice-cold 1 M HCl solution. The formed precipitate was filtered off and subsequently the filtrate was extracted with Et_2O. Afterwards, the organic layers were successively washed with a saturated $NaHCO_3$- and NaCl- solution. The organic layer was dried using $MgSO_4$, filtered off and the solvent was removed under reduced pressure. After purification by vacuum distillation and column chromatography (SiO_2, eluent: heptane) a colourless oil was obtained as pure product (10.60 g; 63 mmol). The purity was checked with ^{1}H-NMR.

Final amount: 10.60 g

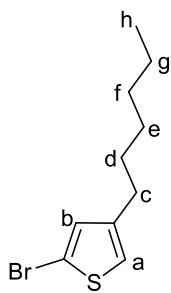Y= 63%

^{1}H-NMR ($CDCl_3$)	δ (ppm)	#H (mp; J)	H?
i h g f e d c b a S	7.22	1 (dd; J = 2.4 Hz; J = 1.8 Hz)	b
	6.90	2 (m)	a, c
	2.56	2 (d)	d
	1.26	8 (m)	e, f, g, h
	0.87	3 (m)	i

5.2.2 Synthesis of 5-bromo-3-hexylthiophene

A solution of *n*-BuLi (11.40 mL; 28.50 mmol) in dry THF (100 mL) at -78 °C, was slowly added to a nitrogen purged solution of tetramethylpiperidine (4.20 g; 29.70 mmol). After stirring for one hour at room temperature, the solution was cannulated to a nitrogen purged solution of 3-hexylthiophene (5.06 g; 30 mmol) in dry THF (20 mL) at -78 °C. This solution reacted for 3 hours at -78 °C, after which a nitrogen purged solution of CBr_4 (13.43 g; 40.50 mmol) in dry THF (100 mL) was added. After a reaction time of 1 hour, the solution was brought to room temperature, after which it was cannulated to water. The organic layers were extracted with heptane and successively washed with a saturated $NaHCO_3$- and NaCl- solution. The organic layer was dried using $MgSO_4$, filtered off and the solvent was removed under reduced pressure. After purification by column chromatography (SiO_2, eluent: heptane), the product was obtained as a colourless oil (2.19 g; 8.84 mmol). The purity was checked with ^{1}H-NMR.
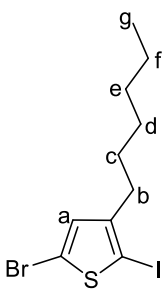
Final amount: 2.19 g

Y= 30%

^{1}H-NMR (CDCl$_3$)	δ (ppm)	#H (mp)	H?
	6.88	1 (s)	a
	6.80	1 (s)	b
	2.54	2 (m)	c
	1.29	8 (m)	d, e, f, g
	0.88	3 (m)	h

5.2.3 Synthesis of 5-bromo-3-hexyl-2-iodothiophene

A solution of 5-bromo-3-hexylthiophene (2.19 g; 8.84 mmol) in DCM (150 mL) was placed under nitrogen atmosphere, shielded from light and brought to 0 °C. After addition of (diacetoxyiodo)benzene (1.42 g; 4.42 mmol) to the stirred solution, I_2 (1.12 g; 4.42 mmol) was gradually added. After overnight stirring at room temperature, the conversion rate was determined via ^{1}H-NMR. The reaction was quenched with $Na_2S_2O_3$. After extraction with heptane, the organic layer was successively washed with a saturated $NaHCO_3$- and NaCl-solution. The organic layer was dried using $MgSO_4$, filtered off and the solvent was removed under reduced pressure. After removal of the solvent, the formed secondary product, iodine benzene, was removed using a vacuum distillation. After purification via column chromatography (SiO_2, eluent: heptane) a pale-yellow oil was obtained (2.01 g; 5.01 mmol). The purity was checked with ^{1}H-NMR.
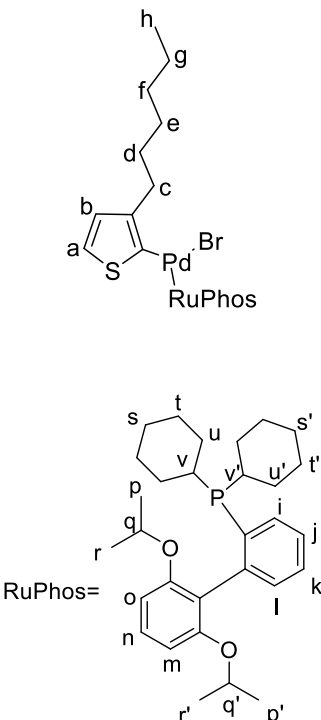
Final amount: 2,01 g

Y= 57%

^{1}H-NMR (CDCl$_3$)	δ (ppm)	#H (mp)	H?
	6.71	1 (s)	a
	2.48	2 (m)	b
	1.31	8 (m)	c, d, e, f
	0.89	3 (m)	g

5.3 Synthesis of the 2-dicyclohexylphosphino-2′,6′-diisopropoxybiphenyl (RuPhos) initiator

A solution of Pd$_2$(dba)$_3$ (0.916 g, 1.00 mmol), RuPhos (0.952 g, 2.04 mmol) and 2-bromo-3-hexylthiophene (1.00 g, 4.00 mmol) in dry toluene (100 mL), was brought under an argon atmosphere, shielded from light and left to react overnight at 60°C. This solution was concentrated under reduced pressure to obtain a few mL of total volume. Afterwards, 50 mL of Et$_2$O was added to the solution and the mixture was filtrated using Celite 545. The filtrate solution was again concentrated under reduced pressure. Afterwards, the reduced volume was added to a 10.0 mL of pentane and it was left overnight into the fridge. The formed precipitate was filtered off and the precipitate was further purified via column chromatography (alumina, eluent= 9.5/0.5 CH$_2$Cl$_2$/EtOAc). The obtained product is a yellow powder.

^{1}H-NMR (CDCl$_3$)	δ (ppm)	#H (mp)	H$_?$
	7,72	1 (t)	j
	7,57	1 (t)	k
	7,40	2 (m)	l, n
	7,29	1 (m)	i
	6.82	2 (m)	m, o
	6,64	1 (d)	a
	6,58	1 (d)	b
	4,57	2 (m)	q/ q'
	2,83	2 (m)	v/ v'
	2,61	2 (m)	c
	2,17	4 (m)	s/ s'
	0,89-1,78	31 (m)	d-h, r/ r', p/ p', t/ t', u/ u'

5.4 Synthesis of the polymers

5.4.1 Synthesis of P3HT

Before polymerization, the precursor monomer, 2-bromo-3-hexyl-5-iodothiophene, was converted to the monomer. Therefore, polymerization tubes were dried in the oven and flushed with nitrogen. To a nitrogen flushed solution of precursor monomer, in dry THF (0.1 M), brought to 0°C, 0.98 equivalents of *i*-PrMgCl·LiCl was added and react for 1h. After 45 minutes of GRIM a ligand exchange of *o*-tolyl-Ni(PPh$_3$)$_2$Br with 2 equivalents of dppp was started. The initiator and the external ligand were weighted in a dry polymerization tube and placed under nitrogen atmosphere. Dry THF (1mL) was added and the solution was stirred for 15 min. After 1 hour of GRIM reaction, the polymerization was initiated by cannulating the monomer solution to the initiator solution and let it react for 1 hour. The quantities used depend on the desired chain length according to the formula DP = [monomer]$_0$/[initiator].

DP	Monomer (mg)	Initiator (mg)	dppp (mg)
13	187	37.7	41.2
15	187	37.7	41.2
24	187	18.9	20.6
28	187	12.6	13.7
37	187	4.71	5.15
41	187	9.43	10.3
45	187	8.38	9.17
55	187	6.28	6.87
70	187	5.80	6.34

0.05 mmol of the GRIM reaction mixture was left into the polymerization tube and quenched with D$_2$O in order to evaluate the conversion with ^{1}H-NMR. After 1 hour of stirring, the polymerization was terminated by the addition of acidified THF.

The polymer was precipitated in MeOH and further purified by a Soxhlet extraction in MeOH and in CHCl$_3$. The chloroform solution was concentrated under reduced pressure and the polymer was precipitated again in MeOH and was filtered off on a glass filter. After the work-up, all the polymers were analyzed by GPC and ^{1}H-NMR.

5.4.2 Synthesis of P3EHT

Before polymerization, the precursor monomer, 2-bromo-[3-(2-ethylhexyl)-5-iodothiophene], was converted to the monomer. Therefore, polymerization tubes were dried in the oven and flushed with nitrogen. To a nitrogen flushed solution of precursor monomer, in dry THF (0.1 M), brought to 0°C, 0.98 equivalents of *i*-PrMgCl·LiCl was added and react for 1h. After 45 minutes of GRIM a ligand exchange of *o*-tolyl-Ni(PPh$_3$)$_2$Br with 2 equivalents of dppp, was started. The initiator and the external ligand were weighted in a dry polymerization tube and placed under nitrogen atmosphere. Dry THF (1mL) was added and the solution was stirred for 15 min. After 1 hour of GRIM reaction, the polymerization was initiated by cannulating the monomer solution to the initiator solution and let it react for 1 hour. The quantities used depend on the desired chain length according to the formula DP = [monomer]$_0$/[initiator].

DP	Monomer (mg)	Initiator (mg)	dppp (mg)
18	201	18.9	20.6
23	201	15.1	16.5
29	201	12.6	13.8
39	201	9.40	10.3
45	201	7.50	8.30
48	201	6.30	6.80
60	201	6.30	6.80
71	201	5.80	6.30
78	201	5.40	5.90

0.05 mmol of the GRIM reaction mixture was left into the polymerization tube and quenched with D_2O in order to evaluate the conversion with ^{1}H-NMR. After 1 hour of stirring, the polymerization was terminated by the addition of acidified THF. The polymer was precipitated in MeOH and was further purified by a Soxhlet extraction in MeOH and in $CHCl_3$. The chloroform solution was concentrated under reduced pressure and the polymer was precipitated again in MeOH and was filtered off on a glass filter. After the work-up, all the polymers were analyzed by GPC and ^{1}H-NMR.

5.4.3 Synthesis of the copolymers of the two regio-isomers of 3-(hexyl)thiophene

Before the polymerization two dry polymerization tubes were flushed with nitrogen. The two precursor monomers, 2-iodo-5-bromo-3-hexylthiophene (M2) and 2-bromo-5-iodo-3-hexylthiophene (M1), were transferred to the polymerization tubes and dried over P_2O_5 under reduced pressure for 4 hours. The amounts of the different reagents for each polymer are shown below. Dry THF was added to the precursor monomers under nitrogen atmosphere to obtain a concentration of 0.1 M, after which a solution of t-BuMgCl (1.63 M, 1 equivalent) was added. The reaction mixture was stirred for 1 hour after which it was cannulated to a dry polymerization tube charged with dry $ZnBr_2$ (dried at 200°C, under reduced pressure).

DP	M1 (mg)	M2 (mg)	Initiator (mg)	ZnBr₂, (M1) (mg)	ZnBr₂, (M2) (mg)
P1	224	0	16.4	207	0
P2	181	6	16.4	183	2.3
P3	177	9	16.4	179	9
P4	168	19	16.4	170	18.8
P5	93.3	93.3	16.4	94.2	94.2

A small part of the GRIM reaction mixture was left in the polymerization tube and quenched with D_2O in order to evaluate the GRIM reaction via ^{1}H-NMR. After a transmetalation of 15 minutes, the right amount of the solutions of the two different monomers were mixed in a polymerization tube. The remaining volume of the starting solution was quenched with D_2O in order to evaluate the transmetalation via ^{1}H-NMR. The mixed solution was added to a solution of the initiator in dry THF (1 mL to start the polymerization After 1 hour, the polymerization reaction was quenched with a solution of acidified THF. The polymer was precipitated in MeOH and was further purified by a Soxhlet extraction in MeOH and in $CHCl_3$. The chloroform solution was concentrated under reduced pressure and the polymer was precipitated again in MeOH and filtered off on a glass filter. After the work-up, all the polymers were again analyzed by GPC and ^{1}H-NMR.

5.5   UV-Vis spectrometry

The Jasco V-730 spectrometer was used to study the aggregation behaviour of conjugated polymers. The spectra were recorded from 300 nm to 750 nm at a data interval of 0.5 nm and a speed of 400 nm/min. A blanco was measured in order to take the cuvette signal and the solvent signal into account.

5.6   Gel permeation chromatography

GPC was used to obtain an estimation of the M_n, M_w and (Đ). The samples were dissolved in THF and filtered over a filter with a pore size of 0.2 μm. The measurements were done on Shimadzu LC20 GPC system with a PL gel 5μm mixed D column. The THF was used as eluent and the references are polystyrene standards.

5.7 Nuclear magnetic resonance spectroscopy

The determination of the purity and chemical structure of the monomers and polymers was done using ^{1}H-NMR spectroscopy. The devices used are a Bruker Avance of 300, 400 MHz.

5.8 Third harmonic scattering (THS)

THS is the used method to measure the second hyperpolarizability of the polymers. Measurements were done in solution in a quartz cuvette with path length of 2mm or 10 mm. A spectra-Physics Insight DeepSee femtosecond pulsed laser with wavelength variation between 700 nm and 1300 nm is used as a high-power light source. The detector is a Bruker Surespectrum 500is spectrometer connected with an EMCCD camera.

ACKNOWLEDGES